The Dissertation Committee for Chung Sub Kim Certifies that this is the approved version of the following dissertation:

Knockdown of HCN1 channels in the dorsal hippocampal CA1 region

Committee:

Daniel Johnston, Supervisor

Richard Aldrich

Michael Mauk

Kimberly Raab-Graham

Eyal Seidemann

Knockdown of HCN1 channels in the dorsal hippocampal CA1 region

by

Chung Sub Kim, B.S.; M. Med. S.

Dissertation

Presented to the Faculty of the Graduate School of

The University of Texas at Austin

in Partial Fulfillment

of the Requirements

for the Degree of

Doctor of Philosophy

The University of Texas at Austin

December 2011

Dedication

My lovely wife, Hyo Sook LIM

Adorable son, David HaEun KIM

and

My entire family for all their love and support

Acknowledgements

First of all, I would like to express my sincere gratitude to my advisor, Dr. Daniel Johnston for providing me with an outstanding research environment. With his guidance, caring, and patience, I can finish my dissertation. I am very lucky to be a member of Johnston lab. I would like to thank the members of thesis committee – Drs. Richard Aldrich, Michael Mauk, Kimberly Raab-Graham, and Eyal Seidemann – for valuable comments and enduring support.

My special thanks goes to Drs. Rick Gray and Randy Chitwood for their excellent support and critical suggestions. Rick and Randy are really talented. Whenever I had some trouble doing research or analysis, they always provided me with the right solution. My research would not have been possible without their helps.

My another special thanks goes to Dr. Payne Chang for valuable and critical comments as well as important contribution. It was my good experience to work with him doing voltage sensitive dye imaging and extracellular field potential recordings. Whenever I had questions about experiment, he always kindly granted me his time to answer and discuss it.

I am very grateful to Drs. Darrin Brager, Nikolai Dembrow, Kevin Dougherty, Brian Kalmbach, and Yul Young Park for their constructive comments, suggestions, and support on this thesis.

I would like to thank graduate students - Ann Clements, Sachin Vaidya, Andrea Dickson – and Dr. Gayathri Nattar Ranganathan for their friendship. Whenever I had good or bad things in the lab, they always cheered me up.

I am grateful to former lab members - Drs. Rishikesh Narayanan, Laurea Diaz, Clifton Rumsey, Stephanie Carlson, Seena Mathew, and Brandy Routh for their support and friendship.

In addition, I would like to thank the administration team - Kathleen Pantalion, Mary Holt, Cynthia Thompson, Susan Cushman Ph.D., and Jason Goltz - for providing invaluable assistance along the way. I also would like to thank Krystal Pho, a graduate coordinator, for providing excellent administrative support and friendship.

I would like to thank the labs of Drs. Mauk, Aldrich, and Raab-Gram for their consistent supports on this thesis, and Dr. Dane Chetkovich (Northwestern University) for HCN1 and HCN2 antibodies and Dr. Paul Pfaffinger (Baylor college of medicine) for the lentiviral vector.

Finally, my truly love and gratitude goes to my family, my lovely wife - Hyo Sook LIM, and my adorable son - David Haeun KIM for their long distance support, prayer, and their best wishes. They made me feel as though I was not alone. Thanks to God!

Knockdown of HCN1 channels in the dorsal hippocampal CA1 region

Publication No._____

Chung Sub Kim, Ph.D.

The University of Texas at Austin, 2011

Supervisor: Daniel Johnston

The hippocampus is an integral brain region for affective disorders. HCN1 protein shows age-dependent increase in expression resulting in an increase in I_h in the dorsal hippocampal CA1 region. TRIP8b knockout mice lacking functional HCN channels as well as both HCN1 and HCN2 knockout mice have been shown to display antidepressant-like behaviors. The mechanisms or brain regions involved in these alterations in behavior, however, are not clear.

We developed a lentiviral shRNA system to examine whether knockdown of HCN1 protein, and therefore h-channels, in the dorsal hippocampal CA1 region is sufficient to produce antidepressant-like effects. We found that silencing of *HCN1* gene resulted in physiological changes consistent with a reduction of I_h and increased cellular excitability of CA1 pyramidal neurons. Rats infused with lentiviral-shRNA-HCN1 in the

dorsal hippocampal CA1 region displayed antidepressant- and anxiolytic-like behaviors. Using voltage-sensitive dye imaging, we found that knockdown of HCN1 in the dorsal hippocampal CA1 region led to enhancement of hippocampal activity in large regions of the dorsal hippocampus.

Our results demonstrate that changed hippocampal network activity by local manipulation of HCN1 channels in dorsal hippocampus led to anxiolytic- and antidepressant-like behaviors and suggest that HCN1 channels could be a potential target for treatment of anxiety and depression.

Table of Contents

List of Tables

List of Figures

Chapter 1:

Introduction

Most neurons receive tens of thousands of synaptic inputs via elaborate dendritic arborizations. Voltage-gated ion channels are non-uniformly distributed in the CA1 pyramidal neurons (Magee 1999) and function to regulate the processing of input information and the induction of plasticity (Frick and Johnston 2005). Of synaptic input to CA1 pyramidal neurons, there are two main sources (Amaral and Witter 1989) : 1) direct sensory information from entorhinal cortex layer III to distal CA1 dendrites in *stratum lacunosum-moleculare* (SLM), 2) Schaffer collateral inputs from CA3 pyramidal neurons to proximal CA1 dendrites in *stratum radiatum* (SR) (Figure 1.1). Membrane currents that are generated by hyperpolarization-activated, cyclic nucleotide gated nonselective cation channels (HCN channels) are characterized by 1) cyclic nucleotide-mediated modulation, 2) Na^+ and K^+ permeability, and 3) activation by membrane hyperpolarization (Pape 1996). In the brain HCN mediated current, called I_h, is important for rhythmic oscillation (McCormick and Pape 1990), synaptic integration (Magee 1998), and the regulation of synaptic transmission (Beaumont and Zucker 2000).

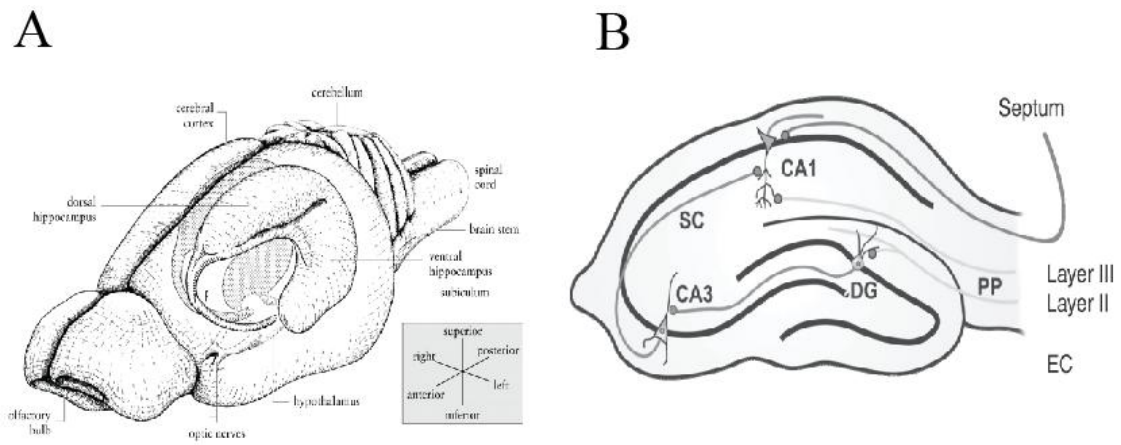

Figure 1.1 Diagram of hippocampus and trisynaptic circuit. (A) Illustration of the rat brain including hippocampus and other brain regions (adapted from Cheung 2005). (B) CA1 pyramidal neurons receive two main synaptic inputs- perforant path synaptic inputs from entorhinal cortex layer III to distal dendrites of CA1 and Schaffer collaterals synaptic inputs from CA3 to proximal dendrites of CA1 region : PP perforant path input, SC Schaffer collaterals input.(adapted from Biel 2009)

Four HCN isoforms (HCN1 ~ HCN4) have been cloned (Santoro, Liu et al. 1998; Monteggia, Eisch et al. 2000). Amino acid sequences in the core transmembrane regions and cyclic nucleotide binding domains (CNBD) are highly conserved by approximately over 80 % (Monteggia, Eisch et al. 2000). The structure of h-channels is composed of six transmembrane segments with a positively charged S4 voltage sensor, a pore forming P region (S5-S6) with GYG signature amino sequences, a cyclic nucleotide binding domain (CNBD), and cytosolic N- and C- terminals (Zagotta and Siegelbaum 1996; Robinson and Siegelbaum 2003) (Figure 1.2).

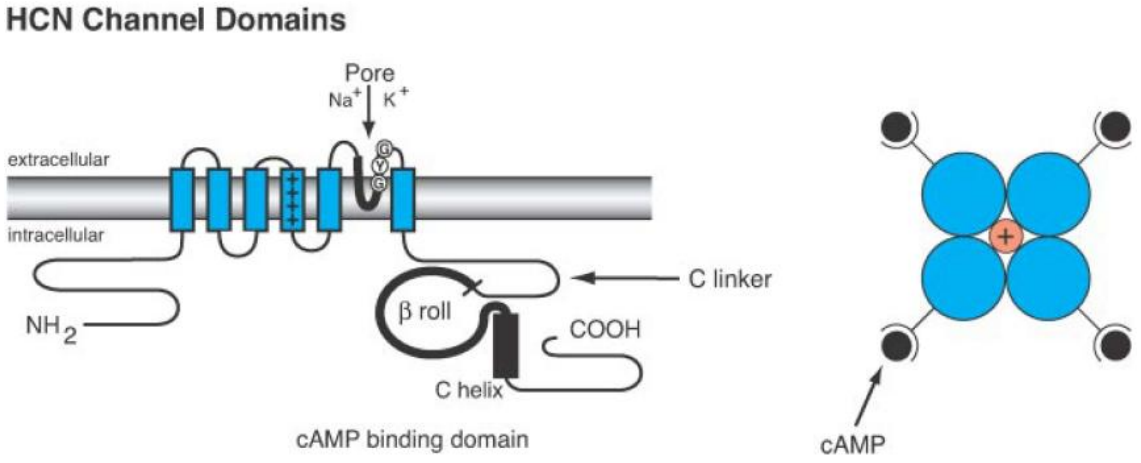

Figure 1.2 Schimetic illustration of HCN channels. HCN channels are composed of six transmembrane regions (S1-S6; blue rectangles) including S4 voltage sensor and pore-forming P-loop with GYG signature amino acid sequence of K^+-selective channels and cytosolic N-/C- terminals. HCN channels are tetrameric with four cyclic nucleotides binding. (Adapted from Robinson 2003)

Tissue distribution of HCN channels (HCN1~HCN4) displays an isoform specific pattern of localization with transcript and protein levels in the brain (Monteggia, Eisch et al. 2000; Notomi and Shigemoto 2004). HCN1 channels are mainly expressed in the hippocampus, neocortex, and cerebellum, whereas HCN2 channels are broadly expressed in the brain (Monteggia, Eisch et al. 2000). In the hippocampus, HCN1 protein is highly expressed in CA1 region rather than CA3 region, whereas HCN2 protein is somewhat more expressed in CA3 region than CA1 region (Brewster, Chen et al. 2007). The amplitude of I_h in the CA1 pyramidal neurons is reduced by about two-third in HCN1 knockout mice (Nolan, Malleret et al. 2003) and one-third in HCN2 knockout mice, respectively (Ludwig, Budde et al. 2003). Various functions of I_h in the brain might be due to different expression patterns of HCN channels (Ludwig, Budde et al. 2003; Nolan, Malleret et al. 2003). In the hippocampal CA1 region, the expression of HCN1

shows a gradient of increasing channel density from the soma to the distal apical dendrites (Lorincz, Notomi et al. 2002) (Figure 1.3A). This is consistent with an increase in I_h density by cell-attached recordings across the somatodendritic compartments (Magee 1998) (Figure 1.3B).

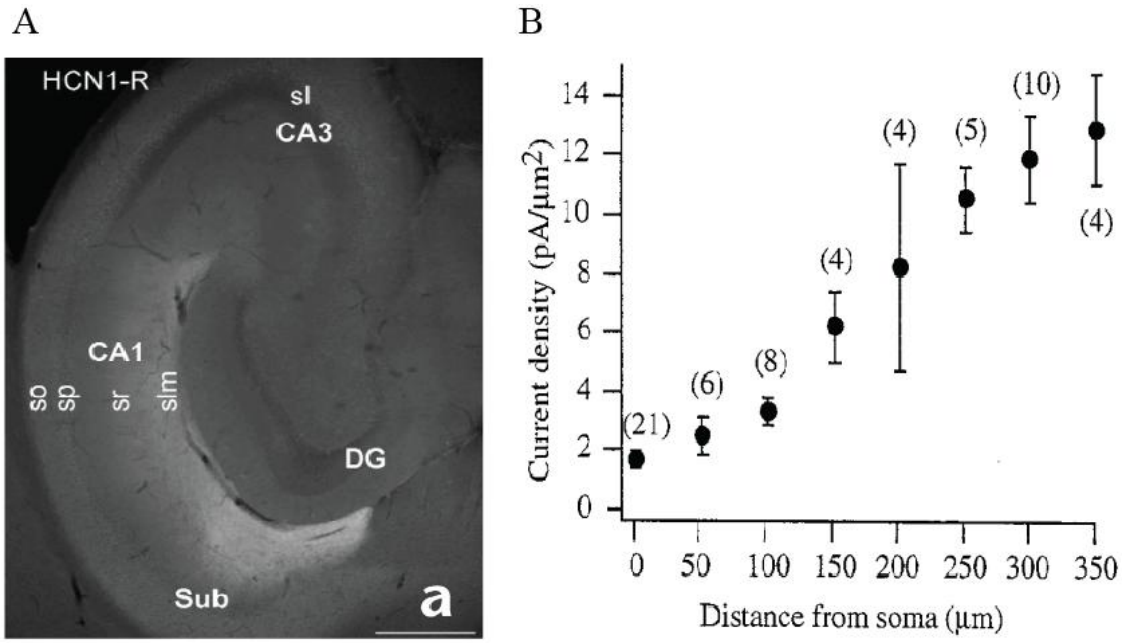

Figure 1.3 Distant-dependnet increase in HCN1 protein expression and I_h density in CA1 region. (A) A gradient of increasing HCN1 protein from the soma to the distal apical dendrites (Adapted from Lorincz 2002). (B) Increase in I_h density across the somatodendritic compartments (Adapted from Magee 1998).

A portion of h-channels are active at rest leading to the generation of a depolarizing non-inactivating inward current and contributing to the resting membrane potential, input resistance (R_{in}), and membrane time constant (τ_m) of CA1 pyramidal neurons (Figure 1.4A). Upon membrane hyperpolarization, there is profound voltage sag resulting from I_h activation which in turn sets the membrane potential back toward its reversal membrane potential (-30 to -40 mV) (Pape 1996). I_h also contributes the intrinsic

resonance properties, which influence how CA1 neurons respond to oscillating inputs (Hu, Vervaeke et al. 2002; Narayanan and Johnston 2007). Blockade of I_h by Cs^+ or ZD7288 enhances αEPSP summation, indicating a key role in the integration of subthreshold synaptic inputs (Magee 1998; Magee 1999) (Figure 1.4 B).

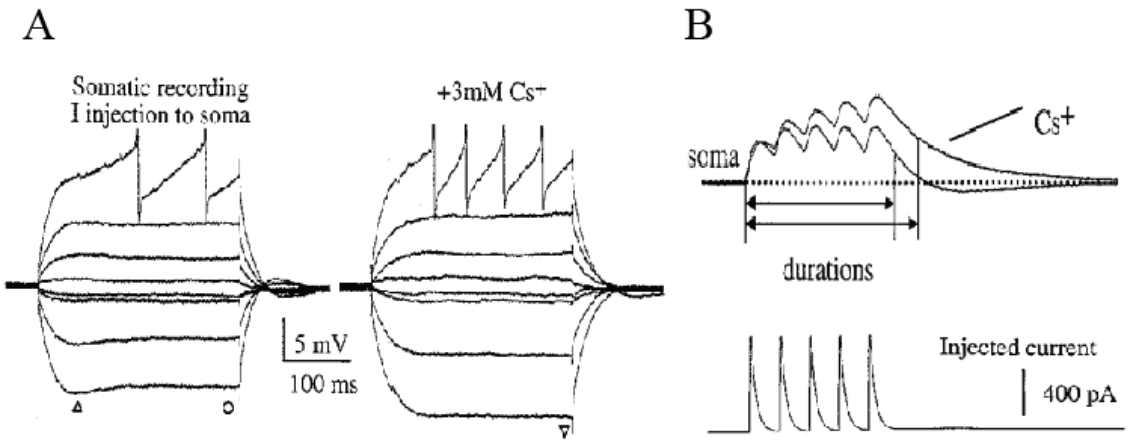

Figure 1.4 I_h-sensitive electrophysiological parameters in CA1 pyramidal neurons. (A) Elimination of voltage sag and increase in input resistant by 3mM CsCl (B) Increase in peak amplitude and duration of EPSP by 3 mM CsCl (Adapted from Magee 1998).

Reduction of functional I_h in the brain resulted in change in behavioral phenotypes (Nolan, Malleret et al. 2003; Nolan, Malleret et al. 2004; Lewis, Vaidya et al. 2011) (Figure 1.5). Global HCN1 knockout mice showed impaired motor learning and memory (Nolan, Malleret et al. 2003), whereas forebrain-specific HCN1 knockout mice displayed improved short- and long-term spatial learning and memory (Nolan, Malleret et al. 2004). Knockdown of *HCN1* gene in the prefrontal cortex (PFC) resulted in improvement of working memory associated with increase in network activity in PFC (Wang, Ramos et al. 2007). In addition, reduction of I_h in three different lines of

knockout mice (TRIP8b, HCN1, and HCN2) showed antidepressant-like behaviors, suggesting that loss of functional I_h might be required for the action of antidepressant-like effects (Lewis, Vaidya et al. 2011).

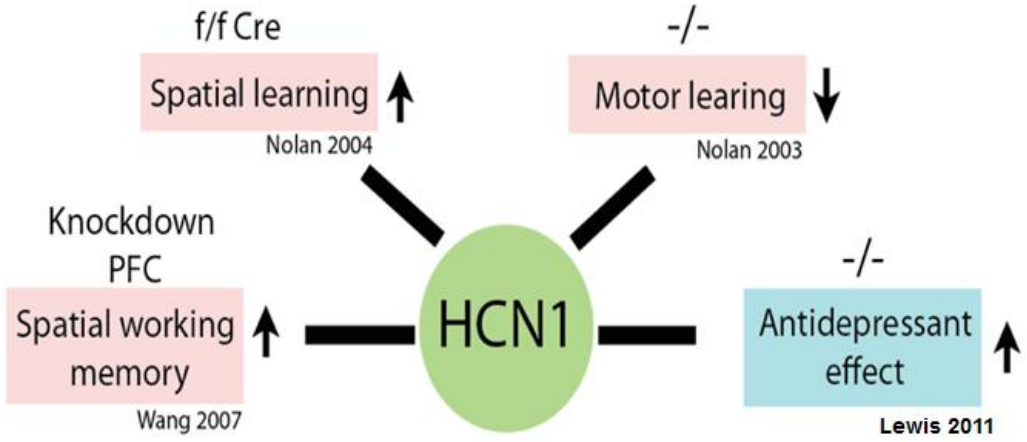

Figure 1.5 Behavioral changes by manipulation of *HCN1* gene. Deletion of HCN1 gene in the brain led to impaired motor learning, wheseas forebrain-specific deletion of HCN1 gene produced improvement of long- and short-term spatial leanring and memory. Knockdown of *HCN1* gene in the PFC resulted in improvement of working memroy.Interestingly, global HCN1 knockout mice displayed antidepressant-like behaivors.

The limbic-cortical system in the brain is considered to be the neural substrate for the action of antidepressants (Mayberg 1997; Mayberg, Brannan et al. 2000). Chronic administration of antidepressant drugs in depressed patients changed regional glucose metabolism measured by positron emission tomography (PET) in the hippocampus (Mayberg, Brannan et al. 2000; Kennedy, Evans et al. 2001) (Figure 1.6). There are several lines of evidence suggesting that dorsal hippocampus is an integral brain region for the action of antidepressants (Padovan and Guimaraes 2004; Lu, Kim et al. 2006;

McLaughlin, Hill et al. 2007). Infusion of leptin, an adipocyte-derived hormone, in the dorsal hippocampus produced antidepressant-like effects leading to induction of c-fos as well as neurogenesis (Lu, Kim et al. 2006; Garza, Guo et al. 2008). Intrahippocampal injection of cannabinoid CB1 receptor agonists or NMDA receptor antagonists reduced immobility time in forced swim test indicating antidepressant-like effects (Padovan and Guimaraes 2004; McLaughlin, Hill et al. 2007). Functional neuroimaging of depressed patients has shown that the volume of posterior hippocampus, which corresponds to the dorsal hippocampus in rodents (Colombo, Fernandez et al. 1998), was significantly reduced (Campbell, Marriott et al. 2004) resulting in impaired spatial learning and memory (Gould, Holmes et al. 2007). It was often observed that patients with depression also have anxiety-like symptoms (Jacobi, Wittchen et al. 2004; Lamers, van Oppen et al. 2011). This comorbidity of depression and anxiety disorders in some patients were effectively treated with chronic administration of fluoxetine (Sonawalla, Farabaugh et al. 2002). In addition, mice chronically subjected with fluoxetine displayed antidepressant- and anxiolytic-like behaviors (Dulawa, Holick et al. 2004), suggesting depression and anxiety might share common neural substrates.

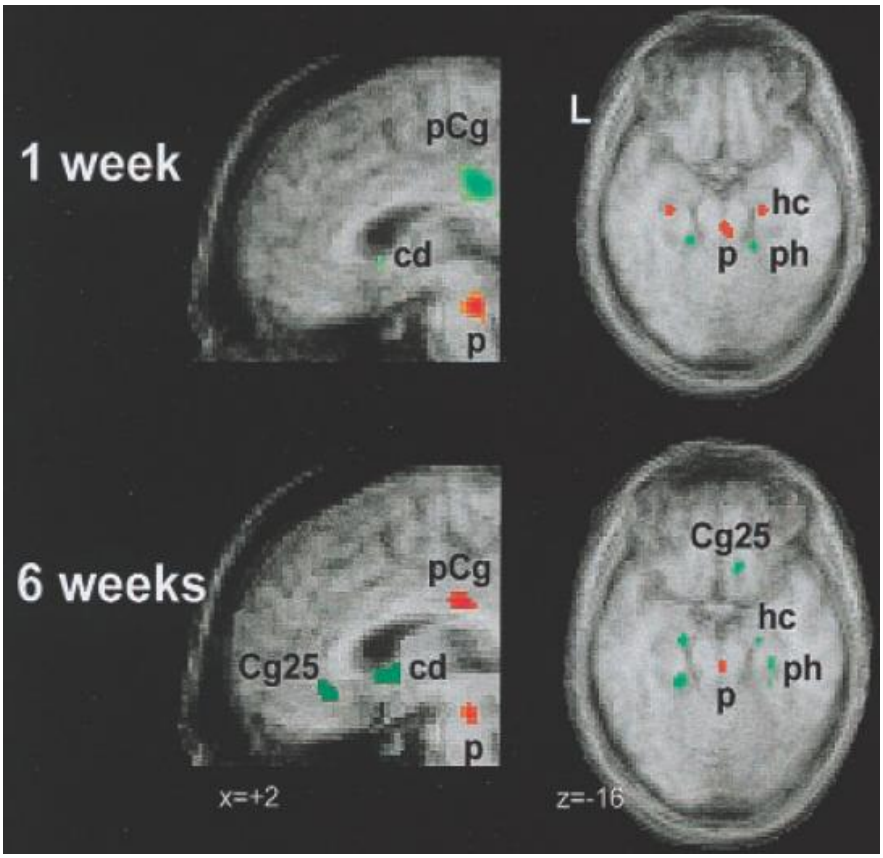

Figure 1.6 Changes in regional glucose metabolism in limbic-cortical areas with time course of fluoxetine effects in depressed patients. Sagittal (left) and axial (right) views. pCg, posterior cingulate; cd, caudate; p, pons; hc, hippocampus; ph, para-hippocampus; Cg25, subgenual cingulate

Although three different lines of knockout mice (TRIP8b, HCN1, and HCN2) resulting in a reduction of I_h and displayed antidepressant-like behaviors, the mechanisms or the brain regions involved were not known. Given the lack of HCN1-specific blockers or genetic animal models that offer region-specific manipulation of HCN1 channels, a lentiviral shRNA system, which provides sequence-specific manipulation with spatial and temporal control was developed (Elbashir, Harborth et al. 2001). RNA interference (RNAi) is a powerful tool for gene silencing. 19-25 nucleotide (nt) small interfering

RNAs (siRNAs) are generated from exogenous double-stranded RNAs (dsRNAs) with enzymatic processing by RNase III-like enzyme called Dicer (Grishok, Pasquinelli et al. 2001). The siRNAs are unwound into single-stranded RNA, resulting in incorporation into RNA-induced silencing complex (RISC). Then, target mRNA is degraded by these complexes, leading to translational repression (Liu, Rand et al. 2003). With this lentiviral shRNA system, it allowed us to investigate the region-specific effects by silencing of *HCN1* gene in the brain.

In this dissertation, I investigated the role of HCN1 channels in the dorsal hippocampal CA1 region. To approach this, full length rat HCN1 was subcloned so as to examine how much HCN1 protein can be reduced by 19 nucleotide shRNA in HEK293 cells. Then lentivirus expressing shRNA against *HCN1* gene was generated in order to determine whether silencing of *HCN1* gene can alter physiological properties in the dorsal CA1 pyramidal neurons. Finally, I have examined how animal behaviors are affected by chronic knockdown of HCN1 protein in the dorsal hippocampus using open field test and modified forced swim test with local manipulation of *HCN1* gene by lentiviral shRNA system. My results indicated that chronic knockdown of *HCN1* gene in the dorsal hippocampal CA1 pyramidal neurons resulted in alterations in intrinsic membrane properties consistent with a reduction in I_h. Furthermore, silencing of *HCN1* gene in the dorsal hippocampal CA1 region produced antidepressant- and anxiolytic-like effects accompanied by enhancement of hippocampal network activity. These findings suggest that targeting *HCN1* gene might provide an alternative therapy for treating depression and anxiety.

Chapter 2:

Materials and methods

Animals. Male Sprague Dawley rats (4-9 weeks-old) were used for these experiments. Rats were housed 2-3 per cage in a temperature (25˚C) and light (12 hour light/12 hour dark cycles) controlled room. All procedures were carried out in strict accordance to the University of Texas at Austin Institutional Animal Care and Use Committee (IACUC).

Drugs. S-ketamine, fluoxetine, and diazepam were obtained from Sigma-Aldrich Co. Diazepam was prepared by dissolving with 0.5% Tween-20 in saline and sonicated.

Construction of lentiviral-shRNA-HCN1. Three shRNA oligos against HCN1 and one shRNA oligo control (non-specific sequence) were designed using web-based software (Genescript) – shRNA-HCN1: CTCAGTCTCTTGCGTTTAT and shRNA-control: TTCAGACTCGTACGTGAAT. Each oligos consists of 19 base-pair sense and antisense sequences, 9 base-pair hairpin loop, TTCAAGAGA sequences, and a poly (T) termination signal. Sense region (5') was attached with *BamH*I restriction enzyme site and antisense region (3') was attached with *Pac*I restriction enzyme site. pLenti-U6-syn-GFP was a gift from Dr. Paul Pfaffinger (Baylor College of Medicine). Each shRNAs oligos were annealed and cloned into *BamH*I (5')-*Pac*I (3') sites (New England Biolabs) of pLenti-U6-syn-GFP vector.

Construction of full length rat HCN1. Rat cDNA was obtained from rat hippocampal CA1 tissue using RT-PCR kit (SuperScript^{TM} II, Invitrogen). Full-length rat HCN1 was generated by general PCR method using following primer sets:

forward primer 5'-CCCAAGCTTATGGAAGGCGGCGGCAAG-3', reverse primer 5'-GGGGTACCTCATAAATTCGAAGCAAAACGG-3'. Forward primers introduced a *Hind*III restriction enzyme site and reverse primers introduced a *Kpn*I site. Amplified full-length rat HCN1 was subcloned into *Hind*III(5') - *Kpn*I(3') sites (New England Biolabs) of pDsRed1-N1(Clontech). Subcloned full-length rat HCN1 was confirmed with sequence and protein expression by western blotting.

Generation of lentivirus. In brief, HEK293T cells were transiently transfected with the pLenti-shRNA plasmid and two helper plasmids (Δ8.9, VSVG) at a ratio of 2:1:1 using $CaPO_4$ transfection method (Nadin and Pfaffinger 2010). HEK293T cells were then grown for two days in DMEM media containing 10% FBS and 1% pen-strep, and then the media containing lentiviral particles were harvested. DMEM media was filtered to remove cell debris using 0.45-μm filter. Concentration and purification with 20% sucrose were performed by ultracentrifugation (Beckman SW-32 rotor) for 2 hrs at 20,000 rpm, at 4^oC.

Stereotaxic microinjection. Stereotaxic surgery was performed under anesthesia with a ketamine/xylazine mixture (90/10 mg/ml). With a 28-gauge stainless steel microinjection cannula (Small Parts, Miami), rats were injected bilaterally with lentivirus expressing

shRNA-control or shRNA-HCN1 into the dorsal hippocampal CA1 region (-3.8 mm anterior posterior, +/- 3.0 mm medial lateral, -2.4 mm dorsal ventral from dura). 1 μl of lentivirus per side was infused for 10 min. After completion of the infusion, the injector was left in place for 5 to 10 min before withdrawal. After stereotaxic injection, rats were returned to their home cages. Body weight was measured after stereotaxic microinjection to monitor recovery.

Western blotting. Western blotting was performed with protein extracted from either wild type CA1 region or lentiviral-infected CA1 region. The protein was separated on 8% sodium dodecyl sulfate-polyacrylamide gel and transferred to nitrocellulose membrane (Invitrogen). Membrane was incubated with blocking solution containing 5% dried milk powder in TPBS (Tween-20 0.1% in PBS buffer) for 1hr. Then the membrane was incubated in primary antibody diluted in blocking solution overnight at 4 ^{o}C. Membrane was rinsed in TPBS buffer 5 x 20 min, and then incubated in secondary antibody for 1hr at room temperature. Primary antibodies were used as following; gp anti-HCN1 (1:1000, from Dr. Dane Chetkovich, Northwestern University), gp anti-HCN2 (1:1000, Dr. Dane Chetkovich, Northwestern University), rabbit anti-tubulin (1:1000, Sigma-Aldrich), and mouse anti-β-actin (1:5000, Sigma-Aldrich).

Immunohistochemistry. Animals were anesthetized and perfused through the ascending aorta using 0.1M PBS followed by 4% paraformaldehyde (PFA) in PBS. The brain was removed and fixed overnight in 4% PFA, and then transferred to 30% sucrose in PBS.

Brains were cut into 50-70 μm coronal sections on a cryostat and stored in cryoprotectant (30% sucrose, 30% ethylene glycol, 1% polyvinyl pyrrolidone, 0.05M sodium phosphate buffer) until processing for immunohistochemistry. Brain slices were briefly rinsed in PBS buffer, and incubated in 0.1% TritonX-100 for 30 min. Subsequently, slices were blocked in PBS solution containing 5 % normal goat serum, 0.03% TritonX-100 for 1hr, and then incubated in primary antibody diluted in blocking solution overnight at 4 ^{o}C. Slices were rinsed in PBS buffer, and then incubated in secondary antibody for 1hr at room temperature. Primary antibody in this study was used as followed; gp anti-HCN1 (1:1000, from Dr. Dane Chetkovich, Northwestern University), gp anti-HCN2 (1:1000, from Dr. Dane Chetkovich, Northwestern University), rabbit anti-GFAP (1:500, Invitrogen), rabbit anti-OSP (1:500, Abcam), rabbit anti-Ferritin (1:500, Abcam), and mouse anti-MAP2 (1:500, Sigma-Aldrich).

Dorsal hippocampal slice preparation and electrophysiology. Animals were bilaterally microinjected with lentivirus expressing shRNA-control in one dorsal CA1 region and shRNA-HCN1 in the other dorsal CA1 region at 4- to 5-week-old rats. Dorsal hippocampal slices (350 μm, coronal section) were prepared from 8- to 9-week-old lentiviral-infected male Sprague-Dawley rats. Then slices were transferred to a holding chamber for 20-30 min at 35^{o}C containing (in mM) 125 NaCl, 2.5 KCl, 1.25 NaH_2PO_4, 25 $NaHCO_3$, 2 $CaCl_2$, 2 $MgCl_2$, 10 dextrose, 1.3 ascorbic acid, and 3 sodium pyruvate, bubbled with 95% O_2 - 5% CO_2. Whole-cell current-clamp recordings were performed on slices submerged in a recording chamber filled with aCSF heated to 32-34 ^{o}C flowing at a

rate of 1 to 2 ml/min in aCSF containing (in mM) 125 NaCl, 2.5 KCl, 1.25 NaH_2PO_4, 25 $NaHCO_3$, 2 $CaCl_2$, 1 $MgCl_2$, and 12.5 dextrose, bubbled with 95% O_2 - 5% CO_2. Lentiviral-infected CA1 pyramidal neurons were visualized using an microscope (Zeiss Axioskop) fitted with differential interference contrast optics and a GFP filter set (Stuart, Dodt et al. 1993). Patch pipettes (4–7 MΩ) were prepared with capillary glass (external diameter 1.65 mm, World Precision Instruments) using Flaming/Brown micropipette puller and filled with an internal solution containing (in mM) 120 K-gluconate, 20 KCl, 10 HEPES, 4 NaCl, 7 K2-phosphocreatine, 4 Mg-ATP, 0.3 Na-GTP (pH 7.3 with KOH). Neurobiotin (Vector Labs) was used (0.1-0.2 %) for subsequent histological processing (DAB staining). Data were acquired with a Dagan BVC-700A amplifier (Dagan, Minneapolis, MN) and were filtered at 3 kHz, sampled at 10 kHz, and digitized by an ITC-18 interface (Instructech Corporation, Port Washington, NY) connected to a computer running custom software written in IGOR Pro (Wavemetrics). Data analyses were also performed with custom software written in IGOR Pro. The experiments were performed under blind conditions. No correction was made for liquid junction potential.

Behavioral procedures. Fifty one rats were assigned into seven groups as follows; Group I: saline i.p. injected (n=13), group II: vehicle (0.5 % Tween-20 in saline) i.p. injected (n=11), group III: ketamine i.p. injected (15 mg/kg, n=9), group IV: Diazepam i.p. injected (1 mg/kg, n=15), group V: Fluoxetine i.p. injected (10 mg/kg, n=9), group VI: lentivirus expressing shRNA-control microinjected into the dorsal hippocampal CA1 region (n=11), group VII: lentivirus expressing shRNA-HCN1 microinjected into the

dorsal hippocampal CA1 region (n=11). All evaluation from behavioral tests was done by a blind experimenter.

- Open field test. The apparatus was consisted of opaque and matte finished black acrylic sheet (36” x 36” x 24”). Each rat was randomly assigned and placed into the center of the field following 30 min saline, vehicle, and diazepam i.p. injection. Behavior in the open field arena was recorded for 6 min using a CCD camera. The surface of the open field arena was cleaned with 70% EtOH in order to remove permeated odors by previous animals after each trial. To analyze behaviors for the last five minutes, the open field arena was divided into 9 equal-size squares (12” by 12”). Basal exploration activity was measured by total travelled distance (inch) and anxiety level was assessed by the number of center square entries, the duration, and the travelled distance in the center square using a custom written program. A line crossing was defined as the body center crosses a line. (Stock, Hand et al. 2001).

- Forced swim test. The tank was made of transparent Plexiglas cylinder (80-cm tall x 30-cm in diameter) filled with water (23–24 ℃) to a depth of 40 cm. Water in the tank was changed after each trial. For the first exposure, rats without drug treatment were placed in the water for 15 min (pre-test session). Twenty-four hours later, rats were placed in the water again for a 6 min session (test session) following 30 min saline, ketamine (15 mg/kg), or fluoxetine (10 mg/kg) i.p. injection. Forced swim test was recorded by a video cameras positioned on the top of the water tank. Behaviors from forced swim test was quantified by using a time sampling technique to rate the predominant behavior over a 5-sec interval as described (Lucki 1997). Passive activity

was defined as floating and making only those movements necessary to keep the nose above the water (Bai, Li et al. 2001; Cryan, Markou et al. 2002).

Voltage sensitive dye (VSD) imaging and extracellular field potential recordings. Animals were bilaterally microinjected with lentivirus expressing shRNA-control in one dorsal CA1 region and shRNA-HCN1 in the other dorsal CA1 region. Dorsal hippocampal slices (400 µm) were prepared from 8- to 9-week-old lentiviral-infected male Sprague-Dawley rats. Slices were stained with the voltage-sensitive dye RH-414 (Molecular probes) for 30 min (0.15 µM in aCSF). Recording pipettes (1-2 MΩ) were filled with aCSF and placed in the stratum radiatum (SR) of the CA1 region. Synaptic responses were evoked by a glass stimulating electrode placed in the stratum radiatum near the border between the CA1 and the CA2 regions. The filter set consisted of a 510-560 nm excitation filter, a 590 nm longpass emission filter, and a 590 nm longpass dichroic mirror. Optical signals were sampled at 1 kHz with a fast CCD camera (CCD-SMQ; RedShirtImaging, GA). Custom software written in C++ was used to control the camera, the amplifier and to analyze the optical and field potential signals. All optical signals were displayed as change in fluorescence divided by resting fluorescence ($\Delta F/F$). The experiments were performed under blind conditions.

Data Analysis. Quantification of data from immunohistochemistry and western blotting was determined by optical density analyses using the ImageJ program. Input resistance was measured by the slope of the linear fit of the V-I plot between +10 and -150 pA

current injection. Rebound slope was measured as the amplitude of the rebound depolarization as a function of the steady-state membrane potential. Voltage sag was calculated as the ratio of the maximum voltage change to the steady-state voltage change resulting from hyperpolarizing current injections. Slow time constant was calculated from a double-exponential fit of the averaged voltage decay resulting from 100 trials of identical 1-ms, 400-pA current injections. Resonance frequency was measured as the frequency of the peak impedance, and resonance strength was the ratio of the peak impedance to the steady-state impedance at a frequency of 1 Hz, using a sinusoidal current injection of constant amplitude and linearly spanning 0-15 Hz in 15 sec. Temporal summation ratio was measured as the amplitude of the fifth αEPSP relative to the first in a train of five αEPSPs at 20 Hz [(αEPSP5 -αEPSP1)/αEPSP1]. Paired-pulse ratio (PPR) was calculated as the ratio of the slope of the second fEPSP to the slope of the first fEPSP. The slope of fEPSP was measured by the initial part of fEPSP (0.5 ms).

Statistical Analysis. All data were expressed as mean ± SEM. The data from whole-cell current-clamp recordings were analyzed using One-way ANOVA. Unpaired t-test was used for the analysis of behavioral results. Two-way ANOVA was used for the analysis of VSD optical signals and field potentials followed by Bonferrori post hoc test. $P<0.05$ was considered as statistically significant.

Chapter 3:

Results

3.1 Development of lentiviral shRNA system.

3.1.1 Knockdown of rHCN1 by pLenti-shRNA-HCN1 in HEK293T cells.

HCN1 protein is highly expressed in several brain areas – neocortex, hippocampus, and cerebellar cortex (Monteggia, Eisch et al. 2000). HCN1 knockout mice showed impairment of motor learning and memory (Nolan, Malleret et al. 2003), whereas forebrain-specific deletion of HCN1 mice displayed improved short- and long-term spatial learning and memory associated with increase of perforant pathway LTP (Nolan, Malleret et al. 2004), indicating that synaptic inputs at distal dendrite of CA1 were constrained by I_h. However, there are no HCN1-specific blockers or genetic animal models that provide region-specific manipulation of HCN1 channels. Furthermore, it has been reported that the expression of HCN protein in the hippocampus is increased with development(Brewster, Chen et al. 2007). To approach this, a lentiviral shRNA system was developed. Lentiviral shRNA vector contains U6 promoter expressing short hairpin RNA (shRNA) and a neuronal promoter, synapsin1 promoter, expressing green fluorescence protein (GFP) (Figure 3.1). Lentivirus promotes the transduction efficiency of RNAi by infecting neurons and long-term expression of transgene in the central nervous system (CNS) (Vigna and Naldini 2000) with non-replicating and self-inactivation (SIN).

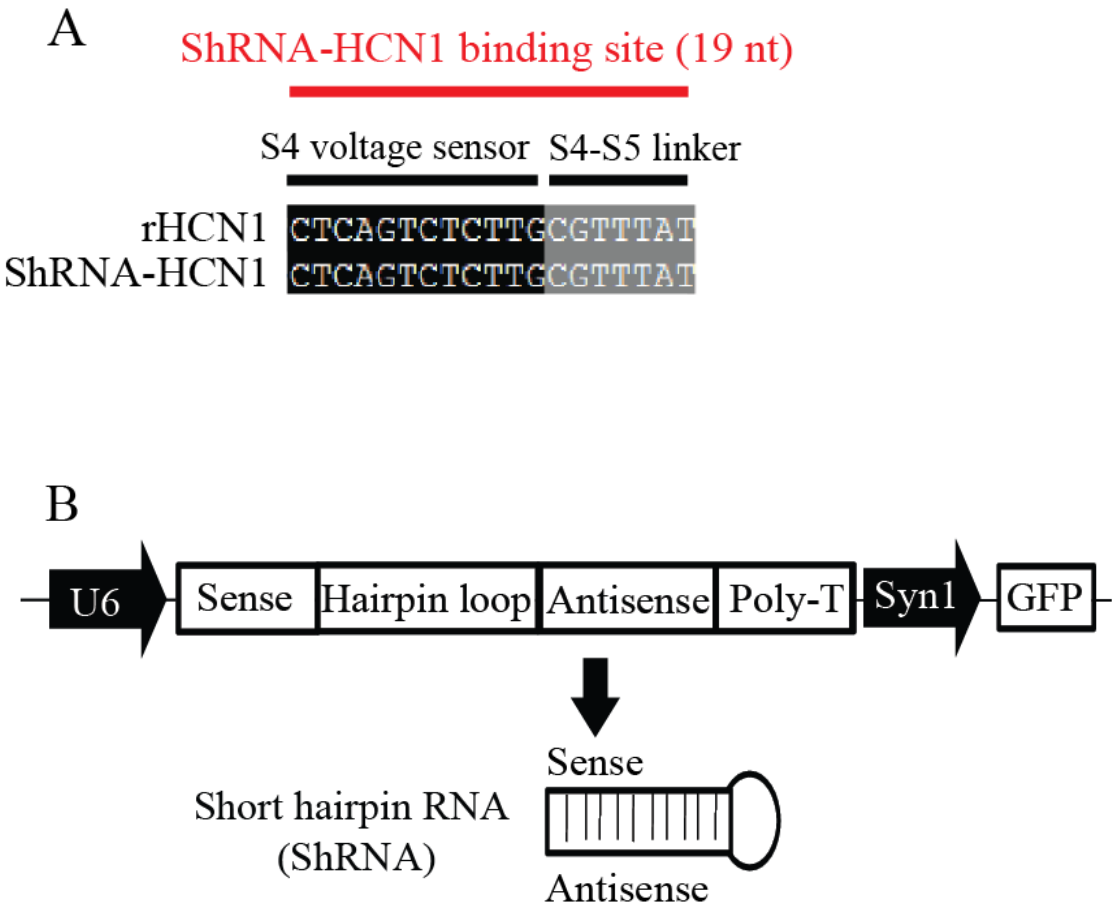

Figure 3.1 Construction of lentiviral shRNA system. (A) The 19 nucleotide shRNA is specific to the rat *HCN1* gene. (B) A schematic diagram showing the lentiviral shRNA expression vector system. In dual promoter vector system, shRNA is under control of U6 promoter and GFP is controlled by synapsin1 promoter, which is a neuron specific promoter.

To determine whether 19 nucleotide shRNA against rat HCN1 can silence rat *HCN1* gene *in vitro*, rat full-length HCN1 was first cloned. Rat full-length *HCN1* gene (NM_053375.1; 2733 base pair) was cloned from hippocampal cDNA using RT-PCR

(Figure 3.2A). Rat HCN1 protein expression was confirmed by western blotting (Figure 3.2B). Then, HEK293T cells were co-transfected with both pLenti-shRNA-HCN1 or pLenti-shRNA-control and pDsRed-rHCN1 at a ratio of 5:1 using $CaPO_4$ transfection method (Chen and Okayama 1988). Red fluorescence protein (RFP) expression was monitored under fluorescence microscope as an index of full-length rat HCN1 protein expression 48 hr after co-transfection, indicating a measurable functional readout. In HEK293T cells that were co-transfected with pLenti-shRNA-HCN1#1 and pDsRed-rHCN1, RFP was dramatically reduced compared to that were co-transfected with pLenti-shRNA-control and pDsRed-rHCN1, suggesting that rat *HCN1* gene was degraded by pLenti-shRNA-HCN1 (Figure 3.2C). Cell lysates were harvested 48hr after co-transfection and performed western blotting. Western blotting analysis revealed that pLenti-shRNA-HCN1 (#1) silenced rHCN1 protein effectively (Figure 3.2D) consistent with degradation of *HCN1* mRNA (Figure 3.2C).

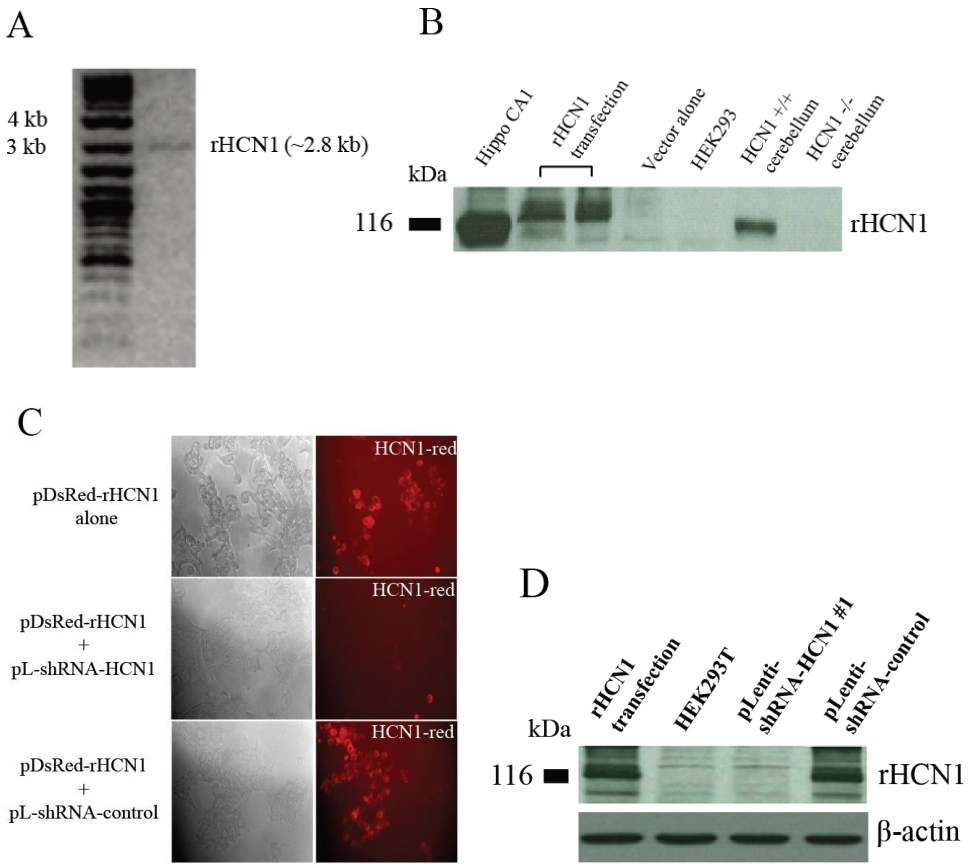

Figure 3.2 Knockdown of rHCN1 by pLenti-shRNA-HCN1 in HEK293T cells. (A) Rat full-length *HCN1* gene was cloned and visualized by gel electrophoresis. (B) Protein was extracted from pDsRed-rHCN1 transfectant HEK293T cells. Rat HCN1 protein expression was confirmed by western blotting. Proteins obtained from hippocampal CA1 and cerebellum tissue (HCN1 wild type) were used as positive controls and from vector (pDsRed) transfectant cells, HEK293T cells, and cerebellum tissue (HCN1 knockout) were used as negative controls. (C) HCN1-Red fluorescence was dramatically decreased by pLenti-shRNA-HCN1#1 compared to pLenti-shRNA-control group, indicating specificity for knockdown of rHCN1. (D) Rat HCN1 protein was significantly reduced by pLenti-shRNA-HCN1 (#1) consistent with silencing of *HCN1* gene.

3.1.2 Lentivirus expressing shRNA in the dorsal hippocampal CA1 region.

Lentivirus expressing short hairpin RNA (shRNA) against HCN1 channels was generated in order to knockdown the expression of HCN1 channels in the dorsal hippocampal CA1 region. Because shRNA expression is driven by U6 promoter, it was confirmed that HCN1 protein is only expressed in neurons and not glia cells (Figure 3.3). Given that the brain parenchyma in young animals has more extracellular space to provide better spread of lentiviral particles (Thorne and Nicholson 2006; Zhao, Keating et al. 2008), 4- to 5-week-old rats were used for infusion of lentivirus in this study. Lentivirus expressing shRNA-HCN1 was infused in the CA1 region of the dorsal hippocampus, which spread mediolaterally (about 0.7 ~ 1.0 mm) and anteroposteriorly (about 1.2 ~ 1.6 mm) (Figure 3.4A) and expressed on 7 days post infusion (DPI) and up to at least six-months (Figure 3.4B), this lentiviral shRNA system, thus, is proper for chronic behavioral study.

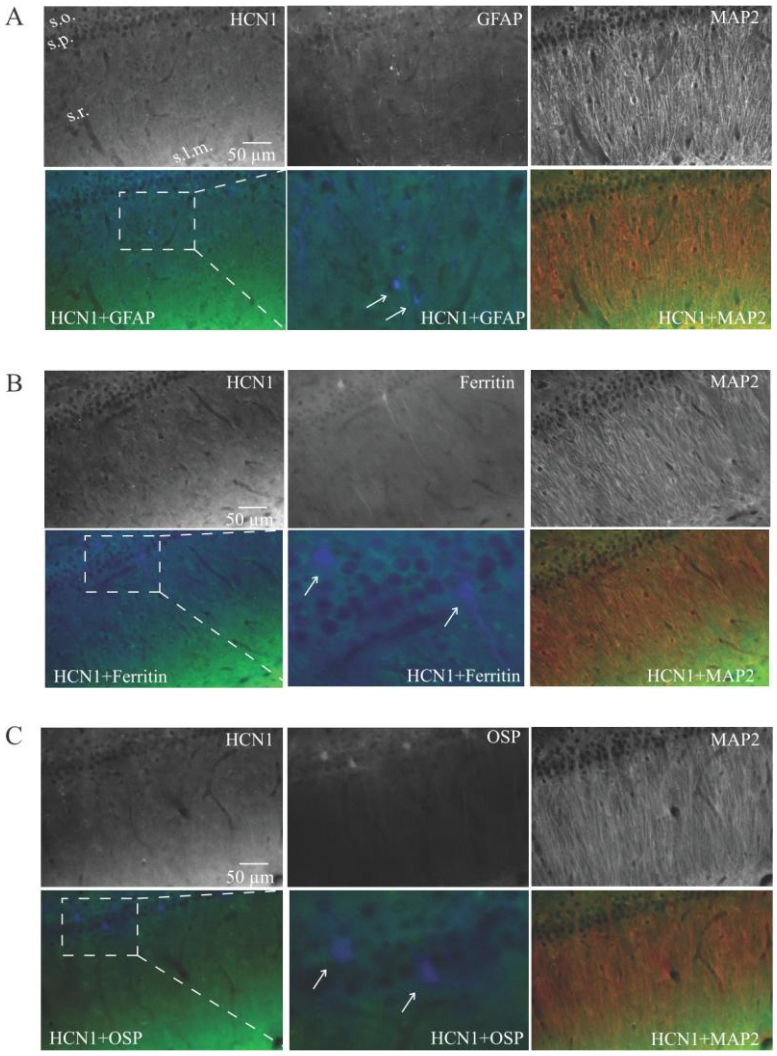

Figure 3.3 Immunohistichemical analysis of HCN1 protein expression in the glia cells. (A-C) 70-μm-thick dorsal hippocampal slices from 8- to 9-week-old rats were immunolabeled with antibodies against HCN1 (Green), dendritic marker MAP2 (Red), astrocyte marker GFAP (A, Blue), microglia marker Ferritin (B, Blue), and oligodendrocyte marker OSP (C, Blue). The arrow indicates astrocyte cell bodies (A), microglia cell bodies (B), and oligodendrocyte cell bodies (C) and enlarged from the dashed box. Z-stack was set at 2 μm.

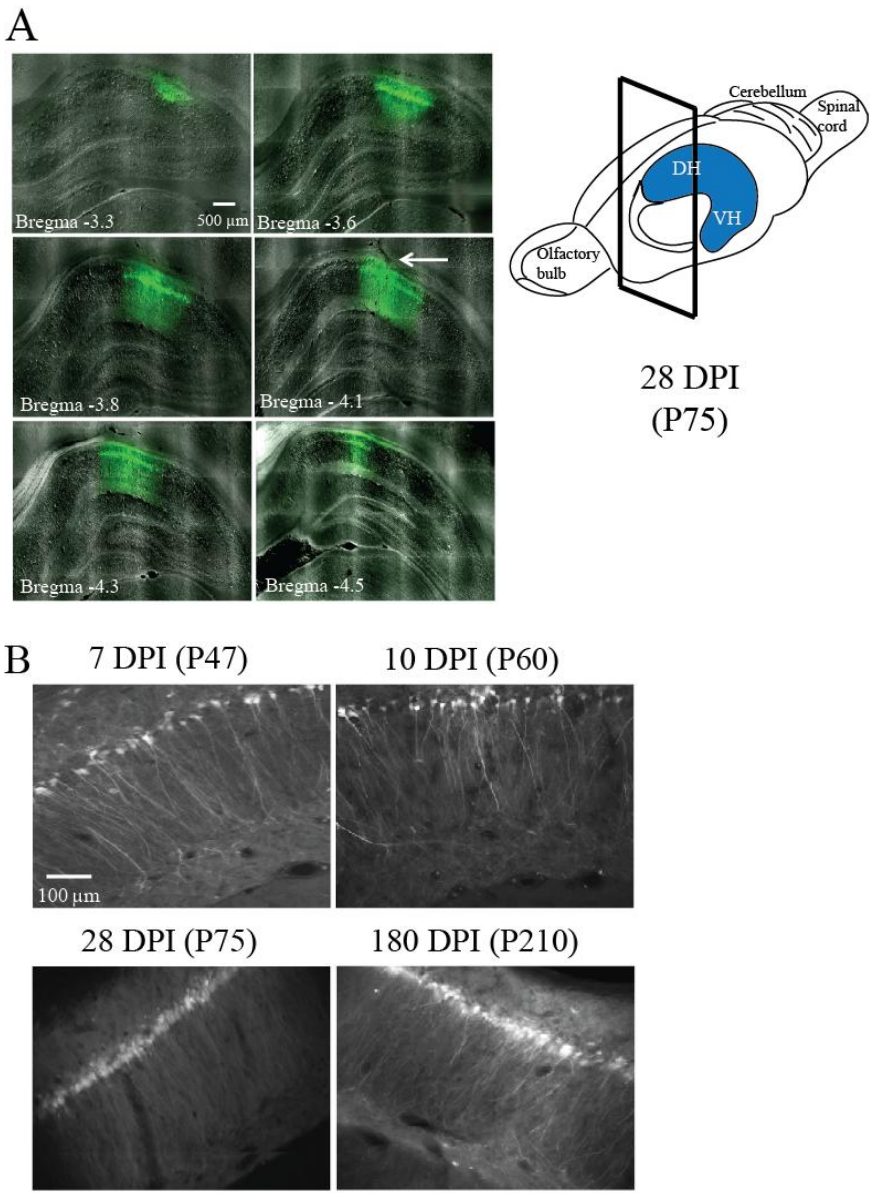

Figure 3.4 Lentivirus expressing shRNA-HCN1 in the dorsal hippocampal CA1 region. (A) Distribution of lentivirus in the dorsal hippocampal CA1 region. A single infusion of lentivirus spread out mediolaterally (about 0.7 - 1.0 mm) and anteroposteriorly (about 1.2-1.6 mm). The arrow indicates the injection track. (B) Expression of lentivirus over time in the dorsal CA1 region. Rats infused with lentiviral-shRNA in the dorsal hippocampal CA1 region were transcardially perfused on day 7, 10, 28, and 180 after infusion (days post infusion, DPI). The ages of animals are in parentheses (postnatal day).

3.1.3 Age-dependent increase in HCN protein expression in the dorsal hippocampal CA1 region.

It has been reported that the expression pattern of HCN1 and HCN2 channels shows developmental-dependent increase in the dorsal hippocampal CA1 region (Brewster, Chen et al. 2007). To confirm this, the level of HCN1 and HCN2 protein was examined by western blotting and immunohistochemistry using specific antibodies against HCN1 and HCN2 channels. Protein was extracted from dorsal CA1 region of individual rats with age (P28, P56, and P112). The protein expression of HCN1 and HCN2 was significantly increased with development (Figures 3.5). The level of HCN1 and HCN2 protein was increased about 35 % and 110 % respectively in young adult rats (P112, n=3) compared to juvenile rats (P28, n=3) (Figure 3.5A) consistent with previous report (Brewster, Chen et al. 2007). Interestingly, HCN1 protein was predominantly expressed in dorsal hippocampal CA1 region of juvenile rats (P28) (Figure 3.5A). Immunohistochemistry results showed that the protein expression of HCN1 and HCN2 was enriched in distal dendrites of CA1 region as well as in perisomatic CA1 region with development (Figure 3.5B).

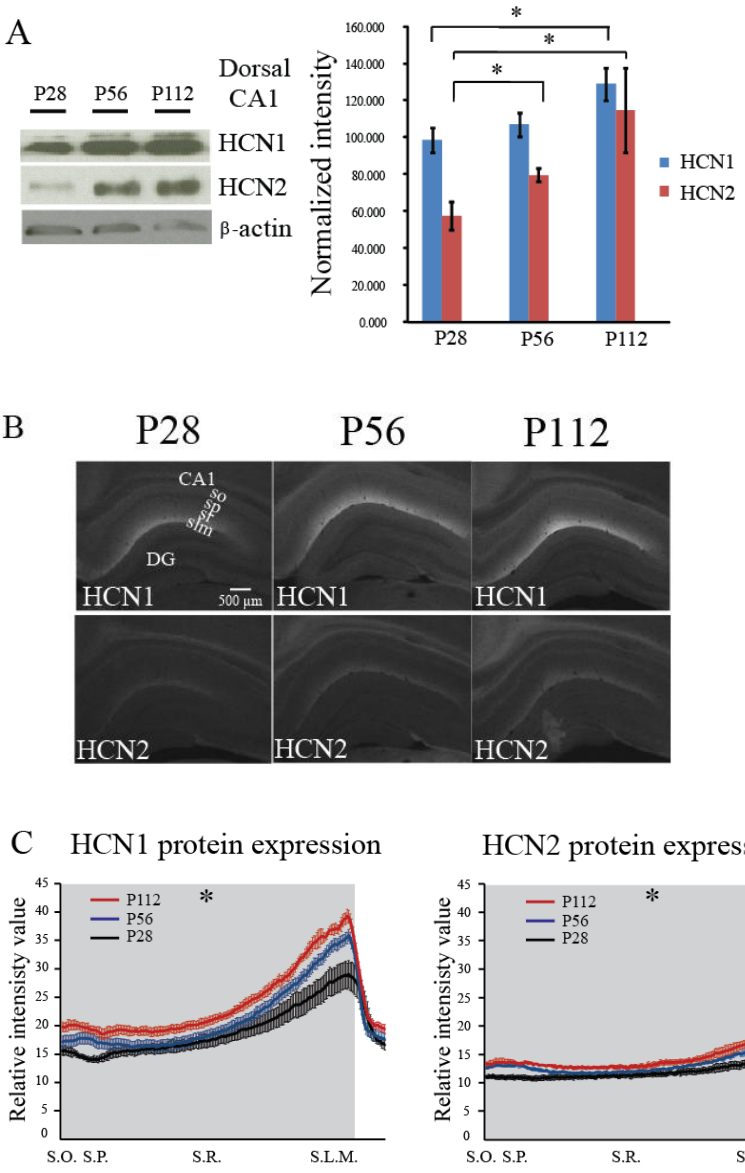

Figure 3.5 Age-dependent increases in HCN1 and HCN2 protein expression in the dorsal hippocampal CA1 region. (A) Western blotting analysis of dorsal hippocampal CA1 lysates of individual different aged rats (P28, P56, and P112; n=3) with antibodies against HCN1, HCN2, and β-actin. The bottom displays the summary of the HCN1 and HCN2 protein expression and was quantified and normalized by β-actin. Data are expressed as mean ± SEM. (B) 50-μm-thick dorsal hippocampal slices from individual different aged rats (P28, P56, and P112; n=3) were immunolabeled with HCN1 and HCN2 antibodies. HCN1 protein was enriched in distal dendrite of CA1 region and was increased with development. HCN2 protein was also increased with age in distal dendrite of CA1 region as well as in perisomatic CA1 region. The bottom showed the quantification of HCN1 and HCN2 protein expression from the perisomatic region to the distal dendritic area in the dorsal CA1 region. Data are expressed mean ± SEM. *$p < 0.05$ compared with juvenile rat group (P28).

3.1.4 Age-dependent change of physiology corresponding to increase in I_h in the dorsal hippocampal CA1 pyramidal neurons.

Because the level of HCN1 and HCN2 protein expression was significantly enhanced with development, it is likely to change physiological properties of dorsal CA1 pyramidal neurons with development. To determine whether age-dependent increase in HCN1 and HCN2 protein expression is correlated with physiological changes in individual dorsal CA1 pyramidal neurons, I_h-sensitive electrophysiological parameters were measured using the whole-cell current-clamp method (Narayanan and Johnston 2007). Dorsal hippocampal slices from juvenile (P28) and young adult (P112) rats were prepared. Dorsal CA1 pyramidal neurons displayed slightly depolarized resting membrane potential (Figures 3.6A and 3.6B), lower input resistance (Figures 3.6A and 3.6C), and longer time-to-peak of sag (Figures 3.6D and 3.6E) compared to juvenile rats group, suggesting alteration in intrinsic membrane properties.

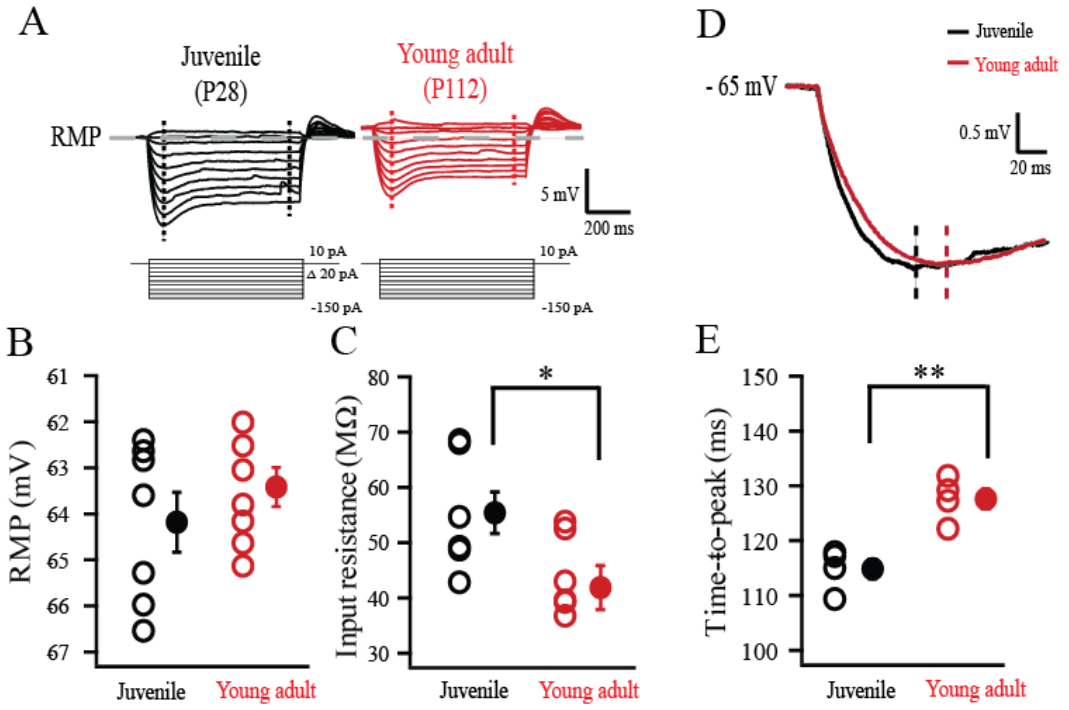

Figure 3.6 Alteration in intrinsic membrane properties with development in the dorsal hippocampal CA1 pyramidal neurons. (A) Representative voltage responses with step current commands ranging from -150 pA to +10 pA (Δ=20 pA) at resting membrane potential. (B) CA1 pyramidal neurons (n=7) from young adult rat group displayed slightly depolarized membrane potential as compared to juvenile rat group (n=7). (C) CA1 pyramidal neurons (n=6) from young adult rat group displayed lower input resistance than juvenile rat group (n=6). (D) Expanded same voltage responses from (A). (E) CA1 pyramidal neurons (n=5) from young adult rat group displayed prolonged time-to-peak of sag compared to juvenile rat group (n=5). Data are expressed as mean ± SEM. *$p < 0.05$ and **$p < 0.01$ compared with juvenile rat group.

For proper comparison between groups, membrane potentials were held at -65 mV with current injection, and electrophysiological properties were compared. Dorsal CA1 pyramidal neurons from young adult rats had higher resonance frequency and strength (Figures 3.7C and 3.7D) compared to juvenile rats group. To examine subthreshold integration, αEPSP summation was measured in response to a train of 5 alpha current injections (α =0.1, 20 Hz) (Poolos, Migliore et al. 2002; Brager and Johnston 2007; Dembrow, Chitwood et al. 2010). Dorsal CA1 pyramidal neurons from

young adult rats group had lower αEPSP summation than juvenile rats group (Figure 3.7E). These electrophysiological results are in general agreement with biochemical results (Figure 3.5).

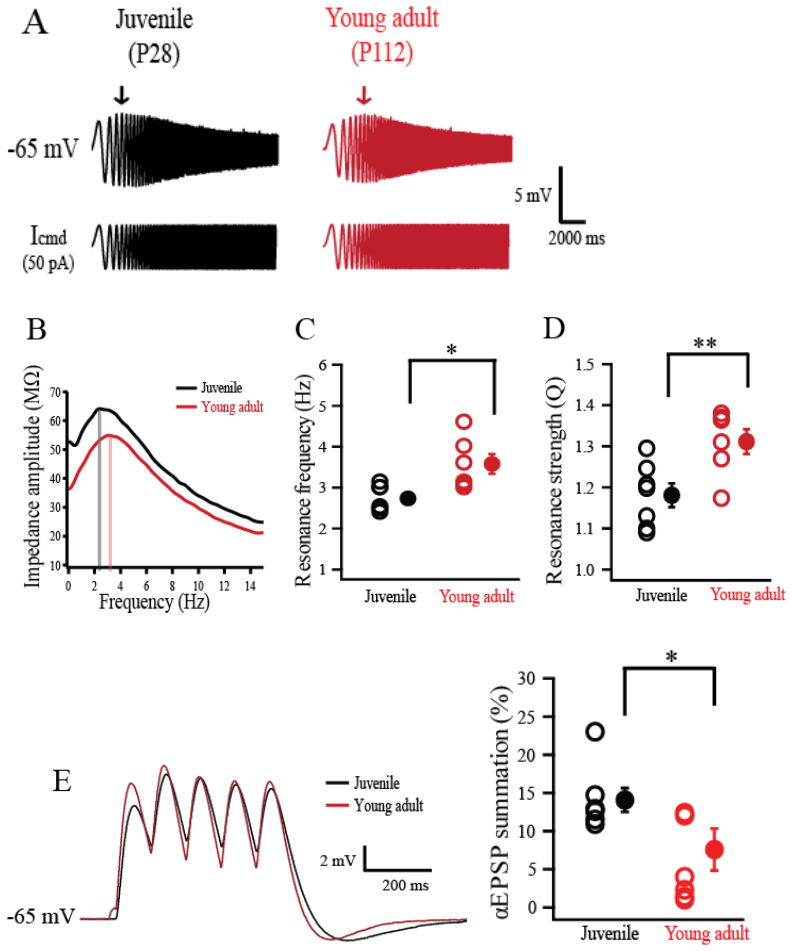

Figure 3.7 Age-dependent induced physiological changes consistent with increase in I_h in the dorsal CA1 pyramidal neurons. For proper comparison between groups, CA1 pyramidal neurons were held at -65 mV. (A) Representative voltage traces and current commands. The arrows point to the maximum depolarization. (B) The profile of the impedance amplitude. The resonance frequencies are marked by vertical lines. (C and D) CA1 pyramidal neurons from young adult rat group (n=7) had higher membrane resonance frequency and strength than juvenile rat group (n=7). (E) Representative voltage traces and current commands. (F) CA1 pyramidal neurons from young adult rat group (n=7) displayed lower αEPSP summation as compared to juvenile rat group (n=7). Data are expressed as mean ± SEM. *$p < 0.05$ and **$p < 0.01$ compared with juvenile rat group.

Table1. I_h-related electrophysiological properties in juvenile and young adult rats (Related to Figures 3.6 and 3.7)

I_h-related parameters	Juvenile group (n=7)	Young adult group (n=7)
RMP (mV)	-64.18±0.64	-63.4±0.42
Input resistance (MΩ)	55.42±3.74 (n=6)	41.8±3.97(n=6)[a]
Time-to-peak (ms)	114.86±1.73 (n=5)	127.6±1.83 (n=5)[b]
Resonance frequency (Hz)	2.73±0.11	3.56±0.24[a]
Resonance strength ratio	1.14±0.03	1.34±0.02[b]
αEPSP summation (%)	14.05±1.55	7.58±2.75[a]

RMP: resting membrane potential. Data are expressed as mean ± SEM. a and b were considered as statistically significant compared to juvenile group

3.2 Knockdown of HCN1 in the dorsal CA1 pyramidal neurons

3.2.1 Quantification of HCN1 protein expression in lentiviral-shRNA-infected dorsal CA1 region by biochemical assays.

To quantify the extent of knockdown of HCN1 channels by lentivirus expressing shRNA-HCN1 in the dorsal hippocampal CA1 region, the level of HCN1 protein was measured by immunohistochemistry and western blotting. The HCN1 protein expression was significantly decreased without alteration of HCN2 and MAP2 protein expression in the infected region as compared to non-infected and shRNA-control-

infected CA1 regions (Figures 3.8A to 3.8D). Quantification of HCN1 protein expression from isolated lentiviral shRNA-HCN1-infected dorsal CA1 region showed a 60% reduction in HCN1 protein expression without change in HCN2 and β-tubulin protein expression as compared to shRNA-control-infected group (Figure 3.8E), suggesting specificity for knockdown of HCN1 channels.

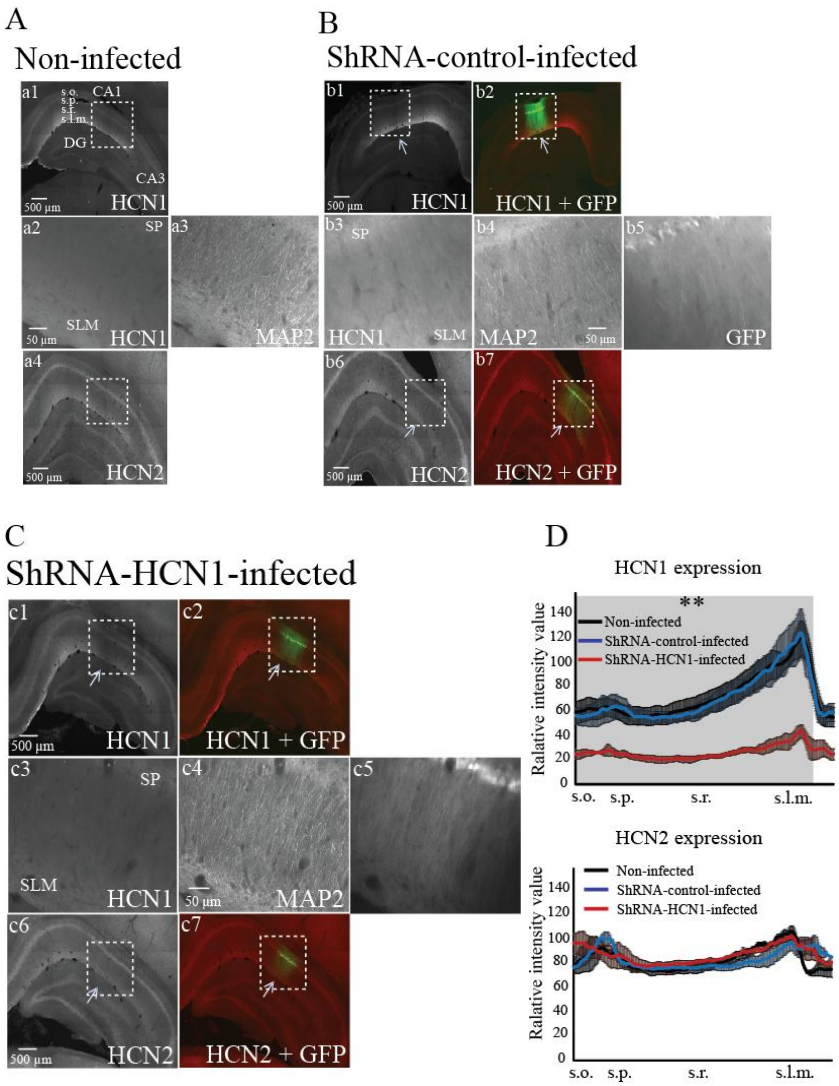

Figure 3.8 Specific knockdown of HCN1 by lentiviral-shRNA-HCN1 in the CA1 region of the dorsal hippocampus.

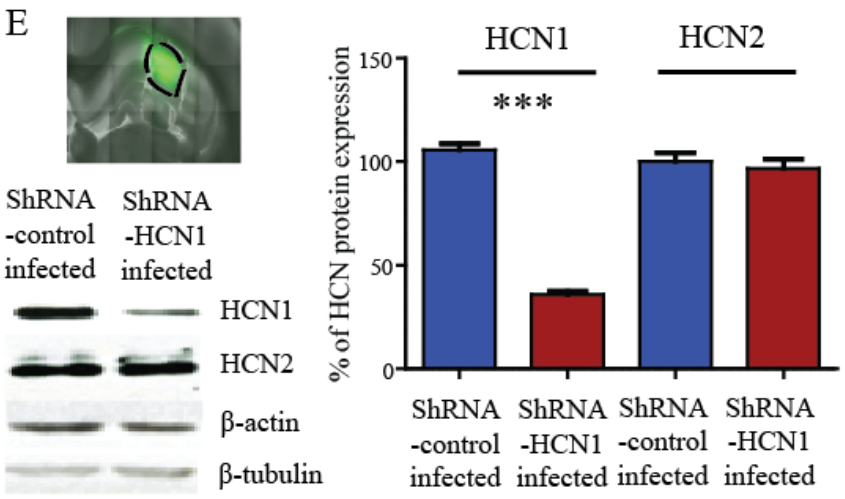

Figure 3.8 cont., Specific knockdown of HCN1 by lentiviral-shRNA-HCN1 in the CA1 region of the dorsal hippocampus. (A) 70-μm-thick dorsal hippocampal slices from non-infected rats were immunolabeled with HCN1 (a1, a2), HCN2 (a4), and dendritic marker MAP2 (a3). a2 and a3 are enlarged from the dashed box. (B) In the shRNA-control-infected dorsal hippocampal CA1 region, protein expression of HCN1 (b1, b3), HCN2 (b6), and MAP2 (b4) were similar to non-infected group. The arrow indicates lentiviral-shRNA-control-infected CA1 region. b3, b4, and b5 are enlarged from the dashed box. The expression of HCN1 (b1) and HCN2 protein (b6) were superimposed with lentiviral-shRNA-control-infected region (b2 and b7). (C) In the ShRNA-HCN1-infected dorsal hippocampal CA1 region, protein expression of HCN1 (c1, c3) was significantly reduced without affecting expression of the HCN2 (c6) and MAP2 (c4). The arrow indicates lentiviral-shRNA-HCN1-infected CA1 region. c3, c4, and c5 are enlarged from the dashed box. The expression of HCN1 (c1) and HCN2 protein (c6) were superimposed with lentiviral-shRNA-HCN1-infected region (c2 and c7). (D) Quantification of HCN1 and HCN2 protein expression from the perisomatic region to the distal dendritic area in the CA1 region (dashed box). The gray shade indicates significant difference in HCN1 protein expression between shRNA-HCN1-infected region and non-infected or shRNA-control-infected regions. There was no significant difference in HCN2 protein expression. (E) Western blotting of lentiviral-shRNA-control-infected (n=4) and lentiviral-shRNA-HCN1-infected (n=4) CA1 lysates with antibodies against HCN1, HCN2, β-actin, and β -tubulin. The protein expression of HCN1 and HCN2 were quantified and normalized by β -tubulin. The right displays the summary of the HCN1 and the HCN2 protein expression in shRNA-control-infected and shRNA-HCN1-infected region. Data are expressed as mean ± SEM. $^{**}p < 0.01$, and $^{***}p < 0.001$ compared with non-infected or lentiviral-shRNA-control-infected group.

3.2.2 Determination of the efficiency of lentiviral shRNA-HCN1 in the dorsal CA1 pyramidal neurons by whole-cell current-clamp recordings.

To determine whether silencing of *HCN1* gene had an effect on the physiology of the dorsal CA1 pyramidal neurons, I_h-sensitive electrophysiological parameters were measured using the whole-cell current-clamp method. Animals were bilaterally microinjected with lentivirus expressing shRNA-control in one dorsal CA1 region and shRNA-HCN1 in the other dorsal CA1 region. Dorsal hippocampal slices (350 μm, coronal section) were prepared from 8- to 9-week-old lentiviral-infected male Sprague-Dawley rats. ShRNA-HCN1-infected CA1 pyramidal neurons had hyperpolarized resting membrane potentials (Figure 3.9C), higher steady-state input resistance (Figure 3.9D), and slower membrane time constant (Figure 3.9E) than non-infected and shRNA-control-infected CA1 pyramidal neurons, suggesting alteration in intrinsic membrane properties.

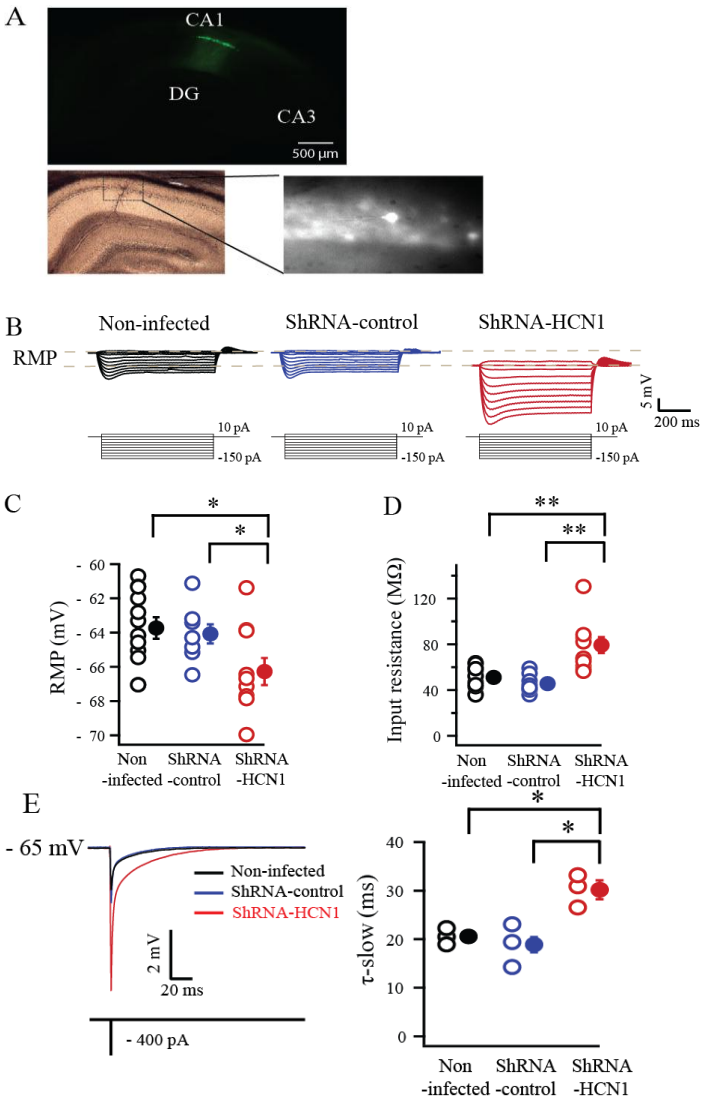

Figure 3.9 cont., Alteration in intrinsic membrane properties by knockdown of HCN1 in the dorsal CA1 pyramidal neurons. (A) Photomicrograph of a representative recorded lentiviral-infected dorsal CA1 pyramidal neurons. The top displays photomicrograph of lentiviral-infected dorsal hippocampal CA1 region. The bottom left displays representative lentiviral-infected CA1 pyramidal neurons, which was visualized by DAB staining after whole-cell current-clamp recordings. The dashed box indicates lentiviral-infected CA1 pyramidal neurons. (B) Representative voltage responses with step current commands ranging from -150 pA to +10 pA (Δ=20 pA) at resting membrane potential. (C) ShRNA-HCN1-infected CA1 pyramidal neurons (n=10) displayed more hyperpolarized membrane potential as compared to non-infected- (n=12) and shRNA-control-infected (n=8) pyramidal neurons. (D) Knockdown of HCN1 in the dorsal CA1 pyramidal neurons (n=10) resulted in higher input resistance than non-infected- (n=12) and shRNA-control-infected (n=8) pyramidal neurons. (E) ShRNA-HCN1-infected pyramidal neurons (n=3) displayed slower time constant compared to non-infected- (n=3) and shRNA-control-infected (n=3) pyramidal neurons. The top displays representative traces and current commands. Lentiviral-shRNA-HCN1-infected neurons were compared with non-infected or lentiviral-shRNA-control-infected CA1 pyramidal neurons. Data are expressed as mean ± SEM. *$p < 0.05$ and **$p < 0.01$.

For proper comparison between groups, we then held membrane potentials at -65 mV with current injection and compared electrophysiological properties. ShRNA-HCN1-infected CA1 pyramidal neurons had less voltage sag (Figure 3.10A), lower resonance frequency and strength (Figure 3.10B) as compared to non-infected and shRNA-control-infected CA1 pyramidal neurons. In addition, shRNA-HCN1-infected CA1 pyramidal neurons displayed more action potentials in response to depolarizing current steps (30 – 300 pA in 30 pA increments for 750 ms) resulting from increased input resistant (R_{in}) by knockdown of HCN1 channels (Figure 3.10C), indicating increased cellular excitability (Shah, Anderson et al. 2004). To examine subthreshold integration, αEPSP summation was measured in response to a train of 5 alpha current injections (α =0.1, 20 Hz) (Poolos, Migliore et al. 2002; Brager and Johnston 2007; Dembrow, Chitwood et al. 2010). ShRNA-HCN1-infected pyramidal neurons had larger αEPSP summation (Figure 3.10D) than non-infected and shRNA-control-infected CA1 pyramidal neurons, resulting from the increased membrane time constant (τ_m) by knockdown of HCN1 channels. These data indicated that knockdown of HCN1 channels by lentiviral shRNA system led to significant physiological changes consistent with a reduction of I_h and an increase in the intrinsic excitability. These results are in agreement with a reduction of HCN1 protein expression by biochemical assays.

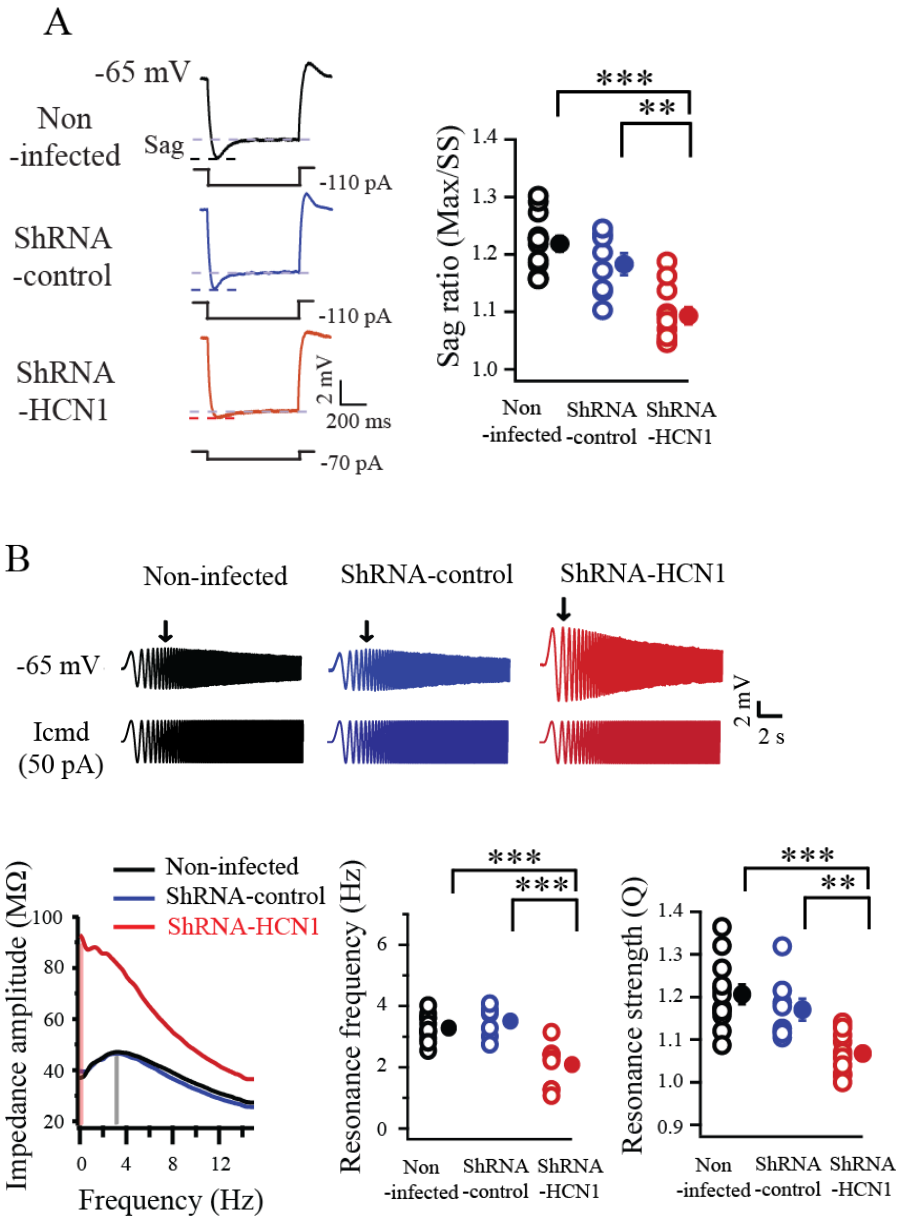

Figure 3.10 Knockdown of HCN1 induced physiological changes consistent with reduction of I_h in the dorsal CA1 pyramidal neurons.

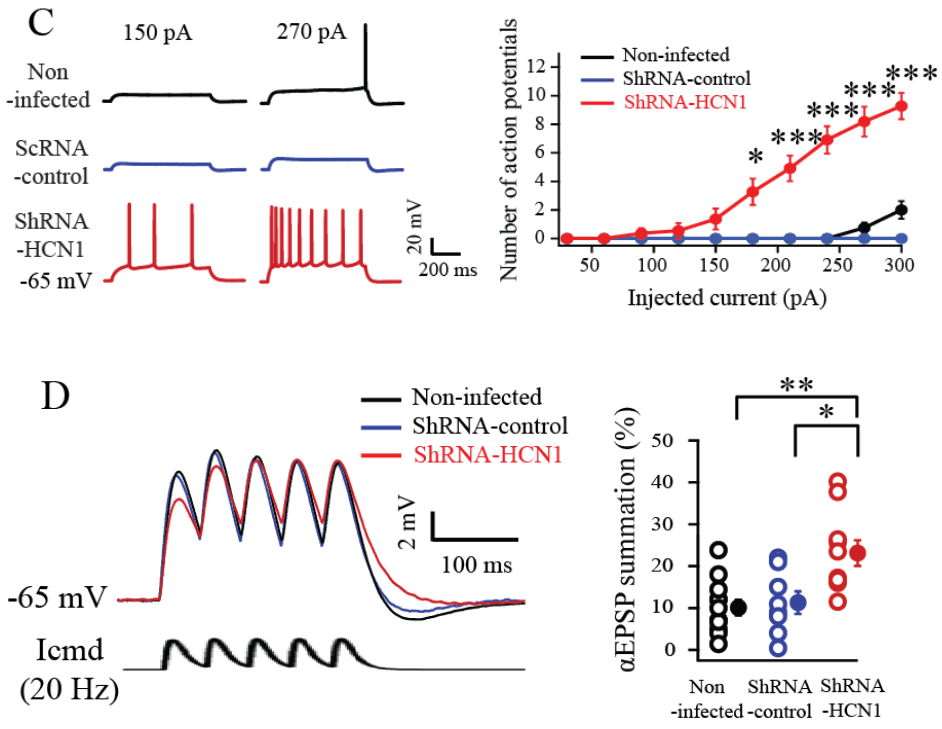

Figure 3.10 cont., Knockdown of HCN1 induced physiological changes consistent with reduction of I_h in the dorsal CA1 pyramidal neurons. For proper comparison between groups, CA1 pyramidal neurons were held at -65 mV. (A) ShRNA-HCN1-infected CA1 pyramidal neurons (n=10) showed less voltage sag compared to non-infected- (n=12) and shRNA-control-infected pyramidal neurons (n=8). The left are representative voltage traces and current commands. The sag is defined as the ratio of the maximum hyperpolarization (Max) to the steady-state hyperpolarization (SS). (B) ShRNA-HCN1-infected pyramidal neurons (n=10) had smaller membrane resonance frequency and strength than non-infected- (n=12) and shRNA-control-infected pyramidal neurons (n=8). The top are representative voltage traces and current commands. The arrows point to the maximum depolarization. The bottom left displays the profile of the impedance amplitude. The resonance frequencies are marked by vertical lines. (C) ShRNA-HCN1-infected pyramidal neurons (n=11) had more action potentials than non-infected- (n=4) and shRNA-control-infected pyramidal neurons (n=3). The top are representative voltage traces and current commands. (D) Knockdown of HCN1 in dorsal CA1 pyramidal neurons (n=10) resulted in higher αEPSP summation as compared to non-infected- (n=12) and shRNA-control-infected pyramidal neurons (n=8). The left are representative voltage traces and current commands. Data are expressed as mean ± SEM. *$p < 0.05$, **$p < 0.01$, and ***$p < 0.001$ compared with non-infected or lentiviral-shRNA-control-infected CA1 pyramidal neurons.

Table 2 Knockdown of HCN1 in the dorsal CA1 pyramidal neurons (Related to Figures 3.9 and 3.10)

I_h-related parameters	Non-infected (n=12)	ShRNA-control-infected (n=8)	ShRNA-HCN1-infected (n=10)
RMP (mV)	-63.73±0.63	-64.07±0.55	-66.27±0.79 [a,b]
Input resistance (MΩ)	45.43±1.90	42.82±1.85	76.15±6.28 [a,b]
Rebound slope (mV/mV)	-0.197±0.014	-0.186±0.018	-0.133±0.014 [a,b]
Voltage sag ratio	1.218±0.0136	1.182±0.0188	1.093±0.0147 [a,b]
Slow τ_m (ms)	20.55±0.48 (n=3)	18.9±1.56 (n=3)	30.18±1.94 (n=3) [a,b]
Resonance frequency (Hz)	3.284±0.12	3.508±0.18	2.09±0.21 [a,b]
Resonance strength ratio	1.20±0.023	1.17±0.025	1.06±0.015 [a,b]
Number of APs (n)[c]	0.75±0.36 (n=4)	0 (n=3)	8.18±1.04 [a,b]
αEPSP summation (%)	10.1±1.83	11.28±2.7	23.13±3.03 [a,b]

RMP: resting membrane potential. AP: action potential. Data are expressed as mean ± SEM. a and b were considered as statistically significant compared to non-infected and shRNA-control-infected groups. c: number of APs in response to 270 pA current injection

3.3 Knockdown of HCN1 in the dorsal hippocampus is sufficient to produce anxiolytic- and antidepressant-like effects

3.3.1 Knockdown of HCN1 in the dorsal hippocampus produced anxiolytic-like effects.

Neuromodulators in the dorsal hippocampus modulate anxiety in various anxiety-related behavioral tests – open field test, elevated plus-maze test, and social interaction test (File, Gonzalez et al. 1998; Degroot, Kashluba et al. 2001; Degroot and Treit 2002). Open field test is a standard behavioral test for investigation of anxiety and basal locomotor activity in rats (Prut and Belzung 2003; Borelli, Nobre et al. 2004; Liu, Garza et al. 2010). In this test, open space acts as a neophobic stimulus, which in turn affects anxiety-induced behaviors and basal locomotor activity (Figure 3.11). Rats subjected in the novel environment displayed less frequency of center entries, less center time and less center distance. These anxiety-related behaviors can be reversed by anxiolytic drugs (Borelli, Nobre et al. 2004; Liu, Garza et al. 2010).

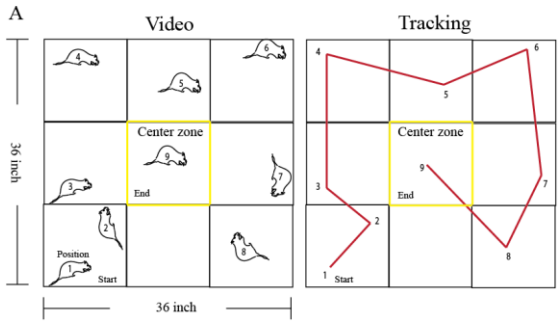

Figure 3.11 Configuration of open field box and video tracking of individual rats. (A) The open field arena was divided into 9 equal-size squares and one center square (12" by 12"). When animal's body center was moving within square or between squares, line was drawing (video tracking). In this example, the number of line crossing is 8 and number of center entries is 1.

As a control experiment, we tested one anxiolytic drug, diazepam, and compared the results with saline- and vehicle-treated rats. Rats that did not receive lentiviral-shRNA infusion were placed into the open field arena 30 min after i.p. injection of saline, vehicle (0.5% Tween-20 in saline), or diazepam (1.0 mg/kg in vehicle solution). Diazepam-treated rats displayed anxiolytic-like behaviors as defined by increased number of center square entries (Figure 3.12D), center square times (Figure 3.12E) , and center distance (Figure 3.12F) compared to saline-treated and vehicle-treated rats, confirming anxiolytic-like behaviors in this behavior paradigm. Rats microinjected with lentiviral-shRNA-HCN1 into dorsal CA1 region displayed increase in number of center square entries (Figure 3.12D), center square time (Figure 3.12E), and center distance (Figure 3.12F) compared to shRNA-control-infected rats. For basal locomotor activity, diazepam-treated rats showed significantly increased locomotor activity (Figures 3.12G and 3.12H), consistent with diazepam-induced hyperactivity (Ennaceur, Michalikova et al. 2010). Like diazepam-treated rats, line crossing (Figure 3.12G), but not total distance (Figure 3.12H), showed significant differences between shRNA-control-infected and shRNA-HCN1-infected rats (Figure 3.12I). Taken together, knockdown of HCN1 in the CA1 region of the dorsal hippocampus promoted anxiolytic-like effects in the open field test.

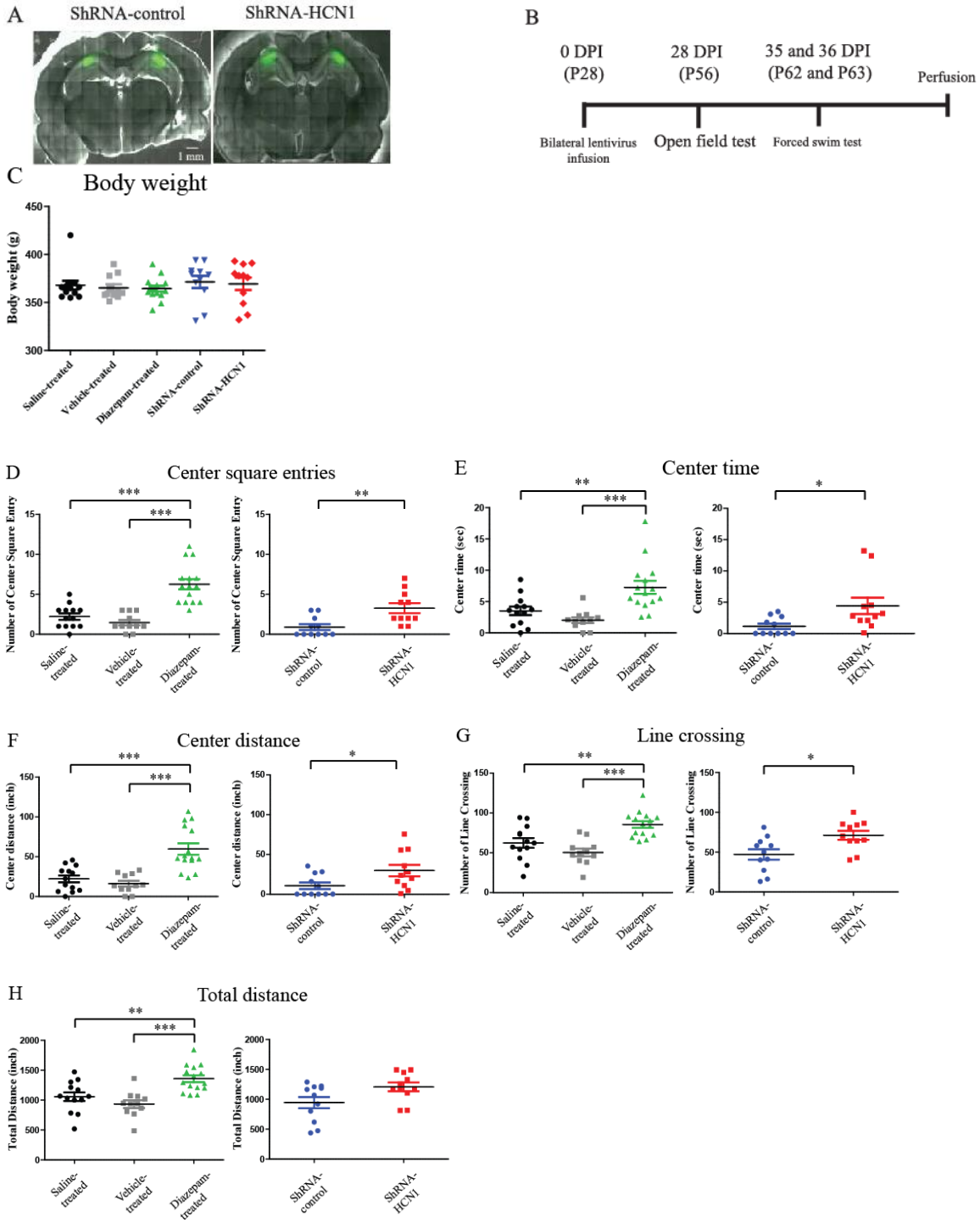

Figure 3.12 Knockdown of HCN1 by lentiviral-shRNA-HCN1 in the CA1 region of the dorsal hippocampus produced anxiolytic-like effect in the open field test (OFT).

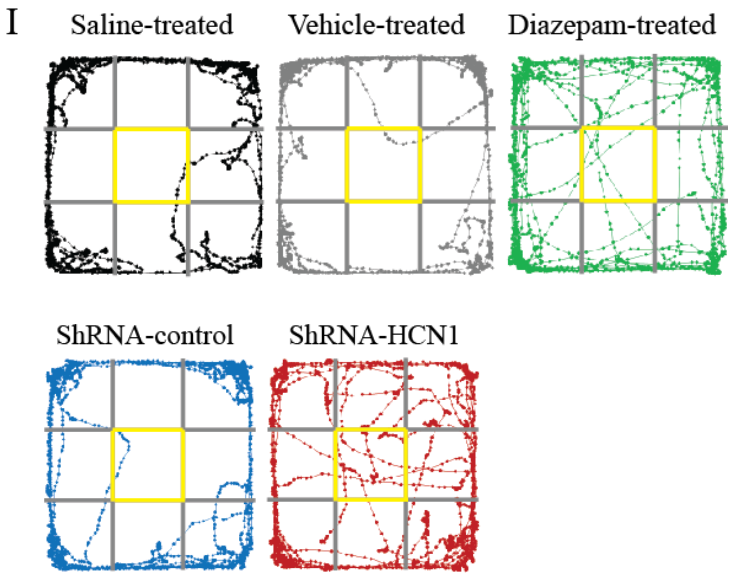

Figure 3.12 cont., Knockdown of HCN1 by lentiviral-shRNA-HCN1 in the CA1 region of the dorsal hippocampus produced anxiolytic-like effect in the open field test (OFT). (A) Representative coronal sections of the brains display the areas infected by lentivirus (green). (B) Rats were microinjected bilaterally with either lentiviral-shRNA-control or lentiviral-shRNA-HCN1 into the dorsal hippocampal CA1 region. OFT was performed on 28 days post infusion (DPI). Age-matched rats were treated with saline (n=13), vehicle (0.5% Tween-20 in saline, n=11) or diazepam (1 mg/kg in vehicle solution, n=15) 30 min before open field test. (C) There was no significant difference in the body weight. (D-F) During the open field test, the number of center entries, center square time, and center distance were measured. Like diazepam-treated rats, shRNA-HCN1-infected rats showed significantly increase in the number of center square entries, center square time, and center distance, indicating anxiolytic-like behaviors compared to shRNA-control-infected rats. (G and H) Like diazepam-treated rats, shRNA-HCN1-infected rats displayed significantly increased basal locomotor activity compared to shRNA-control-infected rats for the last 5 min of the test. There was no significant difference between diazepam-treated group and shRNA-HCN1-infected group. (I) Representative video tracking images of age-matched individual rats treated with saline (i.p. n=13), vehicle (i.p. n=11), and diazepam (i.p. n=15) or lentiviral shRNA-control (infusion in dorsal CA1 region, n=11) or shRNA-HCN1 (infusion in dorsal CA1 region, n=11) during the last 5 min of open field test. Diazepam group was compared with saline or vehicle group (control experiment). ShRNA-HCN1-infected group was compared with shRNA-control-infected group. Data are expressed as mean ± SEM. One-way ANOVA (control experiment) and unpaired t test were performed with significance indicated by $*p < 0.05$, $**p < 0.01$, and $***p < 0.001$.

Table 3 Anxiety and basal locomotor activity in the open field test. (Related to Figure 3.12)

	Saline-treated (n=13)	Vehicle-treated (n=11)	Diazepam-treated (n=15)	ShRNA-control infected (n=11)	ShRNA-HCN1 infected (n=11)
Body weight (g)	368±4.6	365±3.7	364±2.9	371±6.3	369±6.5
Center entries (n)	2.2±0.4	1.4±0.3	6.2±0.6 [a]	0.9±0.3	3.3±0.6 [b]
Center time (sec)	3.5±0.6	2.0±0.4	7.2±1.0 [a]	1.1±0.4	4.4±1.3 [b]
Center distance (inch)	22.2±4.3	16.2±3.5	59.6±7.1 [a]	10.5±4.1	29.6±7.1 [b]
Line crossing (n)	62.0±6.0	50.1±4.7	85.2±4.0 [a]	47±6.6	71.0±5.5 [b]
Total distance (ft)	87.9±6.0	77.7±5.4	113.1±4.7 [a]	78.7±7.9	100.6±5.9 [b]

Data are expressed as mean ± SEM. a was considered as statistically significant compared to saline-treated and vehicle-treated groups. b was considered as statistically significant compared to shRNA-control-infected groups.

3.3.2 Knockdown of HCN1 in the dorsal hippocampal CA1 region produced antidepressant-like effects.

The modified forced swim test (FST) is used to screen antidepressant effects in rats and mice (Lucki 1997). Animals subjected to an inescapable stress environment typically produced two different behavior phenotypes – active activity (swimming and climbing) and passive activity (immobility) (Lucki 1997). Thus, passive activity can be an indicator of behavioral despair in this behavioral paradigm (Porsolt, Bertin et al. 1977). Passive activity is defined as floating and making only those movements necessary to keep the nose above the water (Lucki 1997; Lu, Kim et al. 2006). This

passive activity can be reversed by acute or chronic i.p. injection of clinical antidepressant drugs (Lu, Kim et al. 2006; Liu, Garza et al. 2010). As a control experiment, rats treated with either a sub-anesthetic dose of ketamine (15 mg/kg i.p.) or fluoxetine (10 mg/kg i.p.) displayed significantly reduced immobility time in the forced swim test (Figure 3.13A) compared to saline-treated group, confirming the antidepressant-like effect in this behavioral paradigm. To determine whether knockdown of HCN1 in the CA1 region can produce antidepressant-like effects, age-matched rats were microinjected bilaterally with either lentivirus expressing shRNA-control or shRNA-HCN1 into the dorsal hippocampus. Knockdown of HCN1 was associated with an antidepressant-like effect (Figure 3.13A), whereas shRNA -control-infected animals were not (Figure 3.13A). Because shRNA-infected rats displayed significantly increased horizontal locomotor activity (Figure 3.12G) in the open field test, we further analyzed whether there were positive relationship between locomotor activity and duration of passive activity. We found, however, that there was no correlation between passive activity in FST and basal locomotor activity in OFT (Figures 3.13B), suggesting specificity for antidepressant-like effects by knockdown of HCN1. In addition, diazepam-induced hyperactivity in OFT had no effect on antidepressant effects in forced swim test, suggesting specificity in this behavior test.

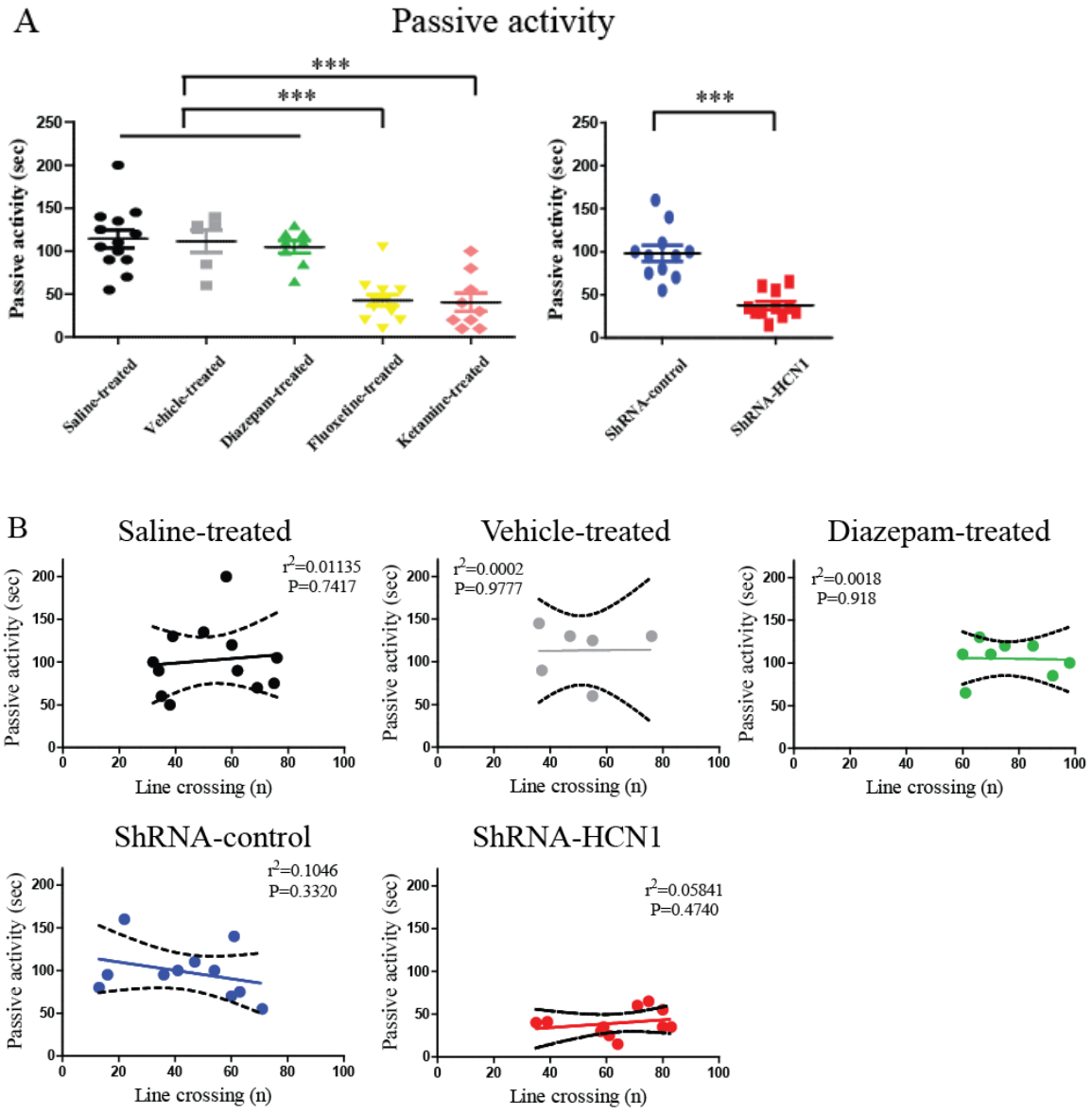

Figure 3.13 Knockdown of HCN1 by lentiviral-shRNA-HCN1 in the CA1 region of the dorsal hippocampus promoted antidepressant-like effects in the forced swim test (FST). (A) As a positive control, rats treated with fluoxetine (10 mg/kg i.p.) or ketamine (15 mg/kg i.p.) displayed significantly less passive activity compared to rats treated with saline (i.p.). Diazepam, an anxiolytic drug, had no effects on antidepressant effect compared to vehicle-treated rats. ShRNA-HCN1-infected rats displayed significantly less passive activity compared to lentiviral-shRNA-control-infected rats. Behavior despair as indicated by duration of passive activity was determined in the last 4 min of the forced swim test. (B) There was no significant correlation between duration of passive activity in the forced swim test and the number of line crossing in the open field test analyzed with linear regression. Data are expressed as mean ± SEM. $*p < 0.05$, $**p < 0.01$, and $***p < 0.001$ compared with non-infected or lentiviral-shRNA-control-infected group.

Table 4 Antidepressant-like effects in the forced swim test (Related to Figure 3.13)

	Passive activity (sec)
Saline-treated (n=13)	114.2±10.2
Vehicle-treated (n=6)	111.6±12.9
Diazepam-treated (n=8)	105±2.8
Ketamine-treated (n=13)	40.5±3.1[a]
Fluoxetine-treated (n=9)	43.0±6.6[a]
ShRNA-control (n=11)	98.1±9.1
ShRNA-HCN1 (n=11)	37.7±4.6[b]

Data are expressed as mean ± SEM. a was considered as statistically significant compared to saline-treated and vehicle-treated groups. b was considered as statistically significant compared to shRNA-control-infected groups.

3.4 Knockdown of HCN1 in the dorsal hippocampal CA1 region led to widespread enhancement of hippocampal network activity

3.4.1 Knockdown of HCN1 in the dorsal hippocampal CA1 region led to widespread enhancement of hippocampal activity by VSD optical imaging.

It has been shown that patients with treatment-resistant depression had pathological activity in the limbic-cortical area by functional neuroimaging, which can be reversed by chronic stimulation of this neural circuit resulting in a reduction of depressed symptoms (Mayberg, Lozano et al. 2005). Animal models of depression induced by chronic mild stress displayed a decrease in the relative activity of DG-CA1 in the hippocampus. This could be reversed by fluoxetine, indicating the significance of

hippocampal network activity in the treatment of depression (Airan, Meltzer et al. 2007). Because knockdown of HCN1 in a small CA1 region of the dorsal hippocampus produced anxiolytic- and antidepressant-like effects, it is possible that chronic knockdown of HCN1 might cause changes in hippocampal network activity. To investigate this, we used voltage sensitive dye imaging in dorsal hippocampal slice from lentiviral-infected rats. A glass stimulating electrode was placed in the stratum radiatum (SR), near the border between the CA1 and CA2 regions to activate the Schaffer collaterals (Chang, Taylor et al. 2007). Both VSD optical signals and extracellular field potentials were recorded in the SR of the CA1 region (Figure 3.14B).

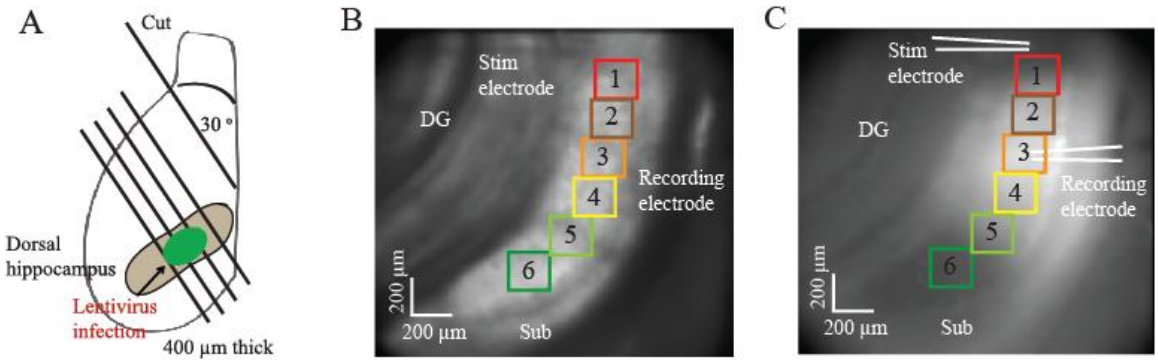

Figure 3.14 Configuration of voltage sensitive dye imaging and extracellular field potential recordings in dorsal hippocampal slice. (A) Schematic illustration of the dorsal hippocampal slices prepared from lentivirus-infected animals. (B) Photomicrograph of a representative hippocampal slice displays the location of the stimulating electrode, the recording electrode, and the regions of interest (ROIs). The size of ROIs is 200 x 200 µm. The Stimulating electrode was placed in the stratum radiatum (SR) close to the CA2 region and the recording electrode was placed in the SR of CA1 region, 500 µm away from the stimulating electrodes. (C) A representative image displays the lentivirus-infected area.

To determine whether knockdown of HCN1 can change hippocampal activity, we used voltage sensitive dye (VSD) imaging in the dorsal hippocampal slices from

shRNA-control- and shRNA-HCN1-infected hippocampi. Knockdown of HCN1 led to enhanced VSD optical signals in response to a burst of stimuli (five 0.2 ms current pulses at 100 Hz, 60 μA and 100 μA) as compared to shRNA-control-infected group (Figure 3.15A), indicating widespread enhancement of hippocampal activity. At the area 500 μm away from the stimulating electrode, where the recording electrode was placed, the peak amplitude of VSD optical signals in shRNA-HCN1-infected slices were significantly larger than those evoked in shRNA-control-infected slices (Figures 3.15C and 3.15D). To compare VSD optical signals in response to a similar number of activated Schaffer collaterals, we grouped data with fixed amplitude of fiber volley (FV, 0.08 mV) and, consistently, the shRNA-HCN1-infected group showed increased VSD optical signals as compared to shRNA-control-infected group (Figure 3.15B). This is consistent with the results from I_h blocker ZD7288 experiment. VSD optical signal was significantly enhanced by I_h blocker 20 μM ZD7288 along the CA1 axis in response to a train of stimuli (five, 0.2 ms current pulses at 100 Hz, 60 μA and 100 μA) (Figures 3.16B-3.16D).

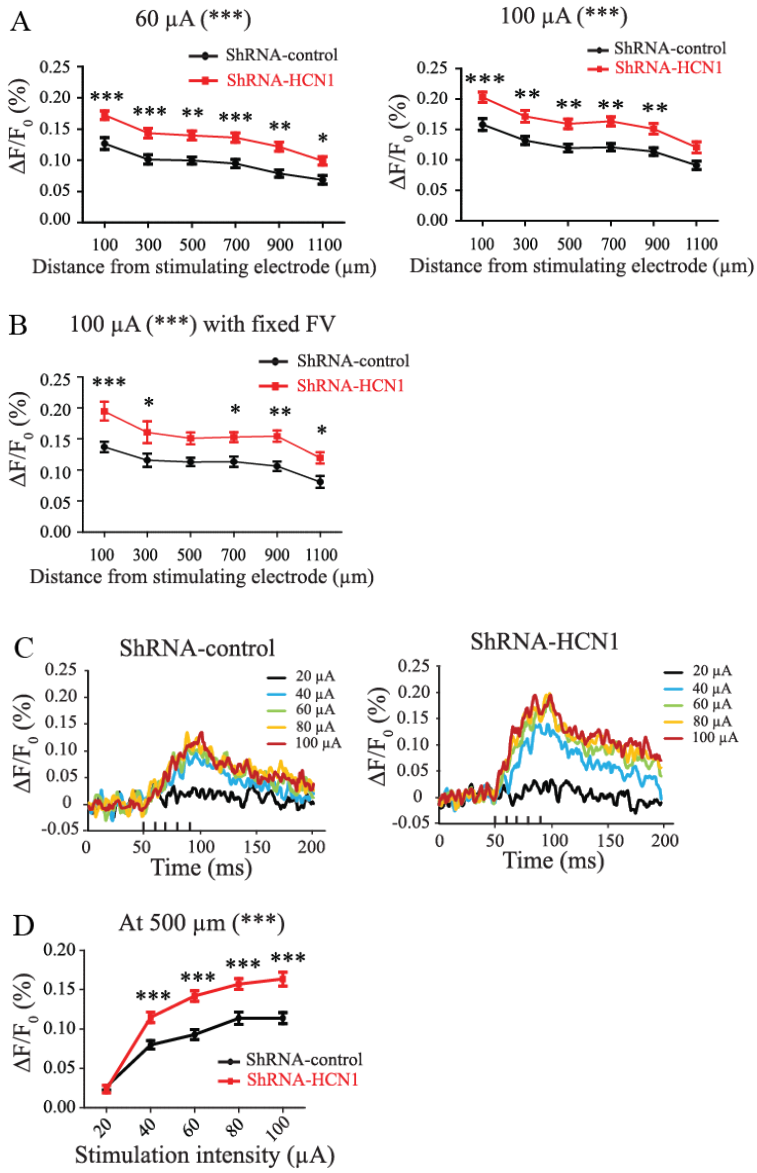

Figure 3.15 Knockdown of HCN1 enhanced voltage sensitive dye (VSD) optical signals in the dorsal hippocampal CA1 region. (A) VSD optical signals were widely increased along the CA1 axis in response to a train of stimuli (five, 0.2 ms current pulses at 100 Hz, 60 µA and 100 µA). (B) Knockdown of HCN1 (n=8) enhanced widespread VSD optical signals with a similar number of activated Schaffer collaterals (0.08 mV) compared to shRNA-control-infected group (n=10). (C) Representative traces of VSD optical signals from the ROIs, 500 µm away from the stimulating electrode, in response to a train of stimuli (five 0.2 ms current pulses at 100 Hz, 20-100 µA). (D) Enhancement of VSD optical signals by knockdown of HCN1 at 500 µm from the stimulating electrode in response to a train of stimuli (five 0.2 ms current pulses at 100 Hz, 20-100 µA). Data are expressed as mean ± SEM. *$p < 0.05$, **$p < 0.01$, and ***$p < 0.001$ compared with lentiviral-shRNA-control-infected group.

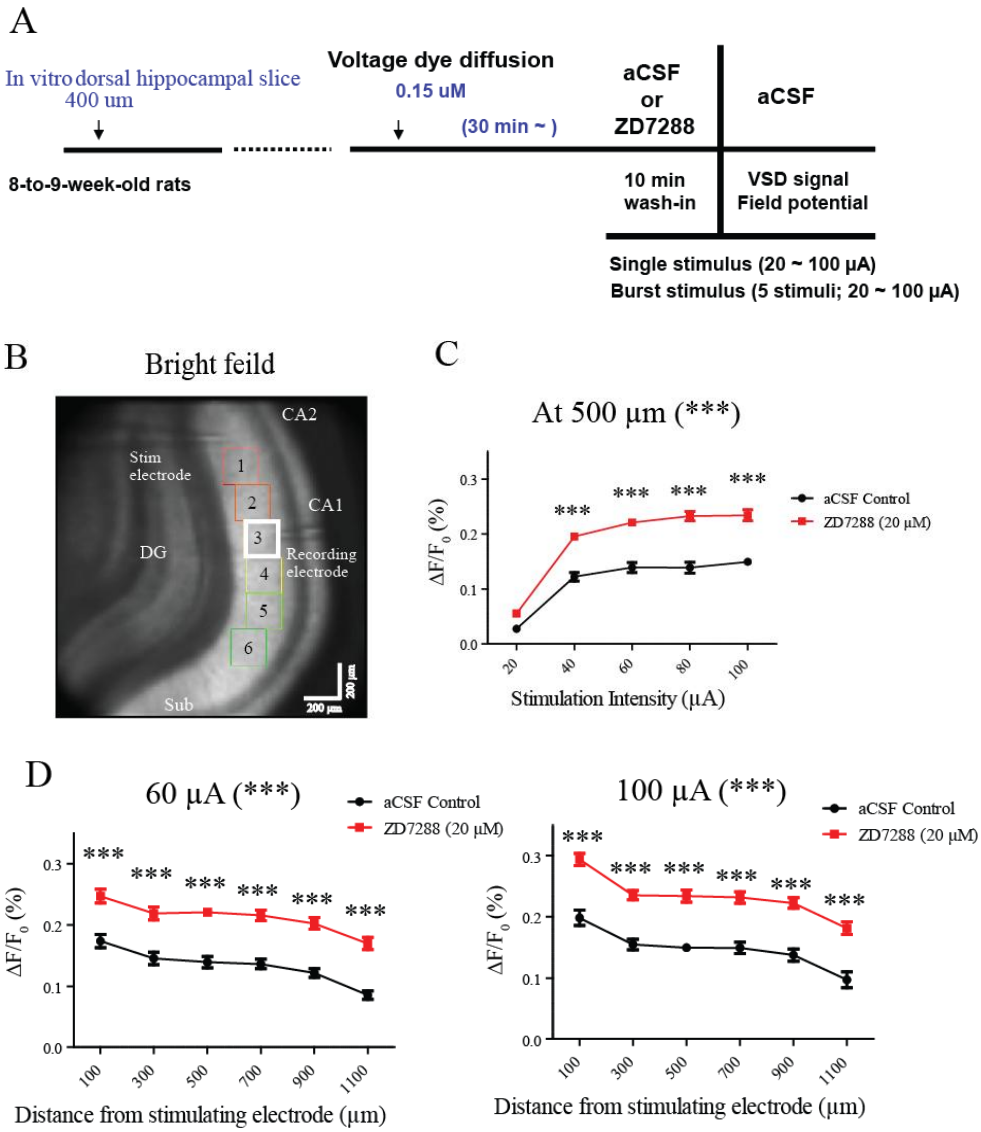

Figure 3.16 Enhancement of voltage sensitive dye (VSD) optical signals by I_h blocker ZD7288 in the dorsal hippocampal CA1 region. (A) *In vitro* dorsal hippocampal slices (400 μm) were prepared from 8-to-9-week-old rats. Slices were stained with the voltage-sensitive dye RH-414 (Molecular probes) for 30 min (0.15 μM in aCSF). VSD optical signal and field potential were determined 10 min after 20 μM ZD7288 was washed into the recording chamber. (B) Configuration of VSD imaging and field potential (See Figure 3.14). (C) Enhancement of VSD optical signals by I_h blocker 20 μM ZD7288 at 500 μm from the stimulating electrode in response to a train of stimuli (five 0.2 ms current pulses at 100 Hz, 20-100 μA). (D) Enhancement of VSD optical signals by I_h blocker 20 μM ZD7288 along the CA1 axis in response to a train of stimuli (five, 0.2 ms current pulses at 100 Hz, 60 μA and 100 μA). Data are expressed as mean ± SEM. ***$p < 0.001$ compared with aCSF control group.

3.4.2 Basal synaptic properties in lentivirus expressing shRNA in the dorsal hippocampal CA1 region.

It has been demonstrated that VSD optical signals reflecting membrane depolarization of postsynaptic neurons were correlated with extracellular field potentials (Tominaga, Tominaga et al. 2000). The widespread enhancement of VSD optical signals in the CA1 region of the dorsal hippocampus from shRNA-HCN1-infected slices suggested that basal synaptic transmission might have been changed. However, there were no significant differences in the slope of field potentials and the amplitude of presynaptic fiber volleys between shRNA-control- and shRNA-HCN1-infected groups (Figures 3.17A to 3.17C). In addition, the paired-pulse ratio (PPR) was not significantly different between shRNA-control- and shRNA-HCN1-infected slices, suggesting no significant difference in presynaptic neurotransmitter release probability between these two groups (Figures 3.17D and 3.17E). On the other hand, the slope of fEPSP was significantly increased by I_h blocker ZD7288 (Figures 3.18A and 3.18C) corresponding to enhancement of VSD optical signal (Figures 3.16C and 3.16D). The amplitude of presynaptic fiber volleys was not changed after ZD7288 treatment (Figure 3.18A and 3.18B). Interestingly, the paired-pulse ratio (PPR) was significantly decreased at 50 ms inter-stimulus intervals (ISI) (Figure 3.18D and 3.18E), indicating increase in the probability of neurotransmitter release.

Taken together, knockdown of HCN1 in the dorsal hippocampal CA1 region resulted in widespread enhancement of VSD optical signals without a change in basal synaptic

properties, whereas blockade of I_h by ZD7288 led to enhancement of VSD optical signals, increase in the slope of fEPSP, and decrease in paired-pulse ratio (PPR).

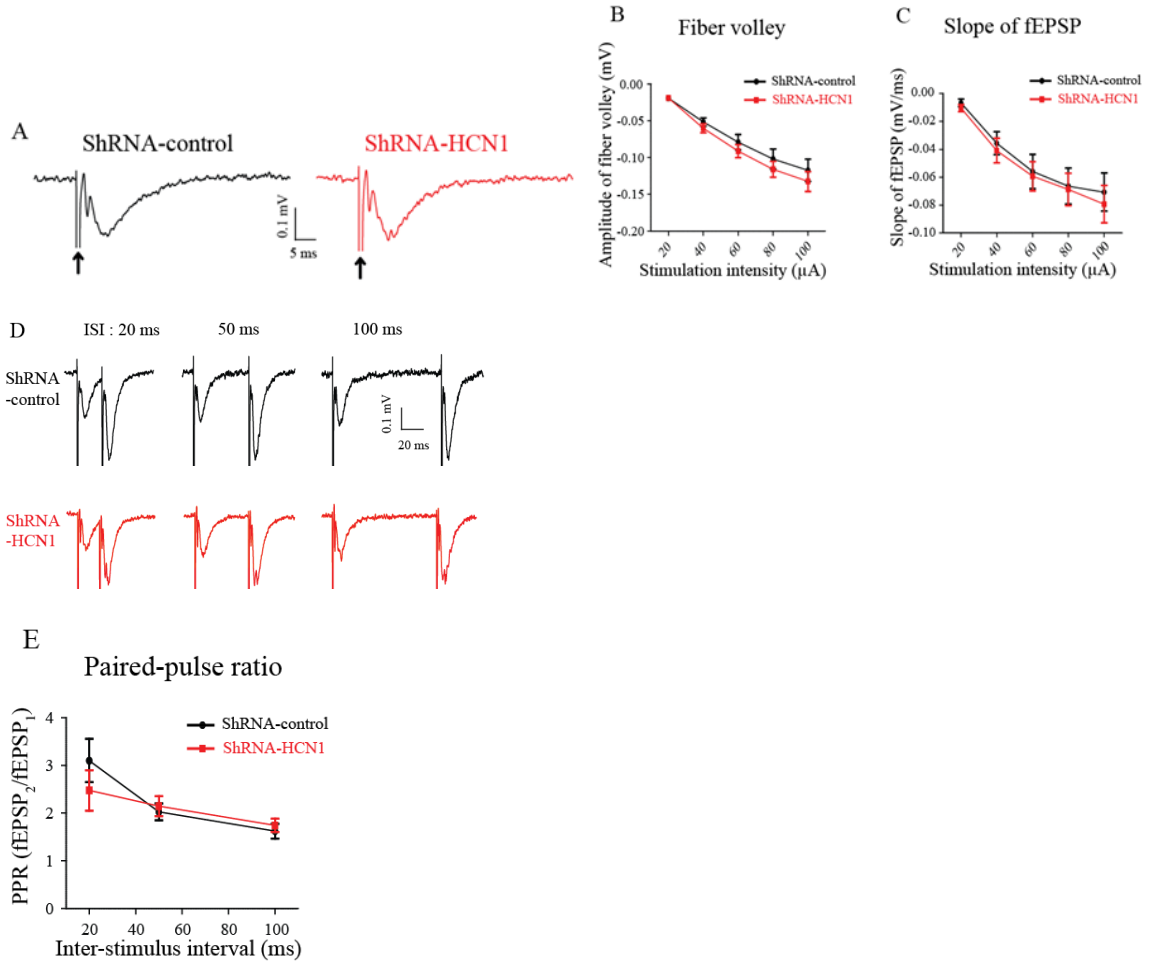

Figure 3.17 Lentiviral-shRNA-control- and lentiviral-shRNA-HCN1-infected dorsal hippocampi had comparable synaptic properties in the CA1 region. (A) Representative traces of fEPSPs from the stratum radiatum (SR) of the CA1 region in response to a single stimulation (100 μA, arrow). (B and C) The amplitude of presynaptic fiber volley and the slope of fEPSP as a function of stimulation intensity from 20 μA to 100 μA showed no significant difference between shRNA-control- (n=18) and shRNA-HCN1-infected (n=18) dorsal hippocampal slices. (D) Representative traces of fEPSPs evoked by paired pulses at three inter-stimulus intervals (ISI; 20 ms, 50 ms, 100 ms) in shRNA-control and shRNA-HCN1-infected dorsal hippocampal slices. (E) Paired-pulse ratios were not significantly different between shRNA-control- (n=10) and shRNA-HCN1-infected (n=10) dorsal hippocampal slices. Data are expressed as mean ± SEM.

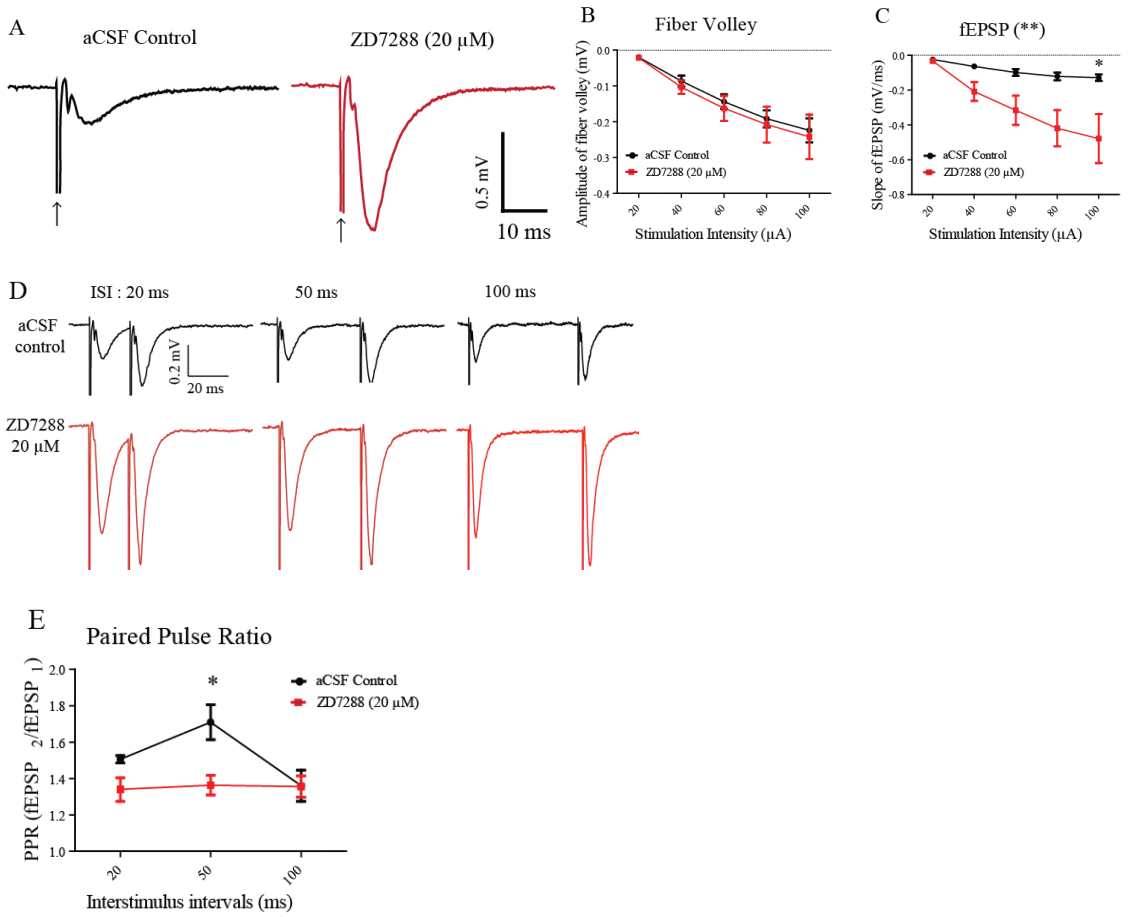

Figure 3.18 Enhancement of basal synaptic transmission by I_h blocker ZD7288 in the dorsal hippocampal CA1 region. (A) Representative traces of fEPSPs from the stratum radiatum (SR) of the CA1 region in response to a single stimulation (100 μA, arrow). (B) The amplitude of presynaptic fiber volley in response to stimulation intensity from 20 μA to 100 μA showed no significant difference between aCSF control (n=6) and 20 μM ZD7288 (n=6). (C) Increase in slope of fEPSP as a function of stimulation intensity from 20 μA to 100 μA by ZD7288 (n=6) compared to aCSF control (n=6). (D) Representative traces of fEPSPs evoked by paired pulses at three inter-stimulus intervals (ISI; 20 ms, 50 ms, 100 ms) in aCSF control and 20 μM ZD7288. (E) Paired-pulse ratio was significantly decreased at 50 ms inter-stimulus intervals. Data are expressed as mean ± SEM. *$p < 0.05$ compared with aCSF control group.

Chapter 4:

Discussion

We used lentiviral shRNA system to locally silence *HCN1* gene in the dorsal hippocampus. Our main findings demonstrate that silencing of *HCN1* gene by lentiviral shRNA-HCN1 resulted in altered physiological properties of individual CA1 neurons, which was sufficient to produce anxiolytic- and antidepressant-like effects in rats. These changes in behavior were accompanied by changes in network activity measured by connections between CA3 and CA1 regions.

Lewis et al. reported that three different lines of knockout mice (HCN1, HCN2, and TRIP8b) with elimination or reduction of functional I_h displayed antidepressant-like behaviors (Lewis, Vaidya et al. 2011). To determine which brain regions may be important for this antidepressant behavior, we developed a lentiviral shRNA-HCN1 system that allowed for focused silencing of the *HCN1* gene. A single infusion of lentivirus expressing shRNA-HCN1 infected about one-third of the dorsal CA1 region and produced a decrease in HCN1 protein expression and physiological changes consistent with the reduction of I_h. Knockdown of HCN1 channels in the CA1 pyramidal neurons led to changes in the intrinsic membrane properties as well as an increase in cellular excitability measured as a change in the number of action potentials elicited by defined current injections.

Anxiolytic- and antidepressant-like effects by knockdown of HCN1 in the dorsal hippocampal CA1 region.

Anxiety- and depression-like symptoms induced by chronic mild stress can be reversed by acute or chronic administration of antidepressant drugs (Lu, Kim et al. 2006; Mineur, Belzung et al. 2006; Liu, Garza et al. 2010). In a clinical study, chronic administration of serotonin selective reuptake inhibitors (SSRIs) showed therapeutic effects in patients with general anxiety disorder (Ball, Kuhn et al. 2005). Our behavioral data showed that knockdown of HCN1 in the dorsal hippocampal CA1 region promoted anxiolytic- and antidepressant-like effects. In the open field test, shRNA-HCN1-infected rats showed significantly increased number of center square entries, duration of center square, and center distance compared to shRNA-control-infected rats. However, TRIP8b and HCN1 knockout mice lacking functional I_h did not display anxiolytic-like behaviors in the elevated plus-maze test and dark/light test (Lewis, Vaidya et al. 2011). It is likely that deletion of *TRIP8b* and *HCN1* genes in the whole brain region might mask or interfere with the anxiolytic-like effects driven by reduction of I_h in the dorsal hippocampus, suggesting a region-specific effect of I_h in other brain regions. A study by Wang et al. demonstrated that knockdown of HCN1 in the prefrontal cortex (PFC) resulted in improved spatial working memory (Wang, Ramos et al. 2007). In addition, forebrain-specific HCN1 knockout mice displayed improved spatial learning and memory, whereas global HCN1 knockout mice showed impaired motor learning and memory (Nolan, Malleret et al. 2003; Nolan, Malleret et al. 2004). These different behavior phenotypes suggest that HCN1 channels expressed in other brain regions

provide different physiological functions. The observation that knockdown of HCN1 in the dorsal hippocampal CA1 region produced antidepressant-like effect in the forced swim test was similar to that previously found from global knockout animals (Lewis, Vaidya et al. 2011). TRIP8b knockout mice lacking functional I_h showed antidepressant-like behavior as indicated by significantly reduced immobility time in forced swim test and tail suspension test without change of basal locomotor activity. This is in general agreement with antidepressant-like effect by knockdown of HCN1 in the dorsal hippocampal CA1 region. However shRNA-HCN1-infected rats showed significantly increased number of line crossing compared to shRNA-control-infected rats, indicating increased basal locomotor activity. Linear regression analysis from behavior results confirmed that there were no correlation between locomotor activity and duration of immobility, suggesting specificity for antidepressant-like effect by knockdown of HCN1.

Widespread enhancement of hippocampal activity by knockdown of HCN1 in dorsal CA1 region.

Why does knockdown of HCN1 in a small CA1 region of the dorsal hippocampus produce anxiolytic- and antidepressant-like effects? It has been shown that chronic electrical stimulation in limbic-cortical region from patients with treatment resistant depression reduced pathological metabolic activity, which in turn produced therapeutic effects, implying that alternation in limbic-cortical activity may be involved in this treatment of severe depression (Mayberg 2003; Mayberg, Lozano et al. 2005). In a functional neuroimaging study, patients with severe depression showed reduced posterior

hippocampal volume, suggesting that there might be a concomitant impairment of spatial learning and memory (Campbell and Macqueen 2004). Indeed, depressed patients showed deficits of spatial learning and memory by virtual navigation task as compared to healthy subjects (Gould, Holmes et al. 2007). In non-clinical study, Airan et al. showed that animal model of depression induced by chronic mild stress displayed alteration in relative activity of DG-CA1 using voltage sensitive dye imaging, which can be reversed by an antidepressant drug, indicating that modulation of hippocampal network activity might be required for the treatment of depression (Airan, Meltzer et al. 2007). Consistent with these findings, knockdown of HCN1 in the dorsal hippocampal CA1 region resulted in widespread increase of VSD optical signals in response to afferent stimulation, indicating an enhancement of dorsal hippocampal activity. This enhanced VSD optical signal is consistent with the effects of I_h blocker ZD7288, showing enhancement of VSD optical signal. Knockdown of HCN1 showed no difference of the slope of fEPSP, whereas bath application of I_h blocker ZD7288 resulted in increase in the slope of fEPSP reflecting enhancement of VSD optical signal. This discrepancy might be due to different amounts of change in membrane potential and input resistance between shRNA-HCN1 and I_h blocker ZD7288. In whole-cell current-clamp recordings, shRNA-HCN1-infected CA1 pyramidal neurons had about -3 mV membrane hyperpolarization and an increased in steady-state input resistance (about 60 %) compared to non-infected and shRNA-control-infected groups. This is similar to the results from CA1 pyramidal neurons infected by shRNA-TRIP8b (Piskorowski, Santoro et al. 2011). With these changes in membrane potential and input resistance, theoretical calculation and computer simulation

give us about 26% increase in the size of EPSPs (measured by VSD imaging), but only about 3% increase in the amplitude of synaptic current (measured by field potential recordings) in response to our simulation protocol (data not shown). Because we observed change in behavior phenotypes by knockdown of HCN1 channels in a small CA1 region of the dorsal hippocampus, it is possible that lentivirus-shRNA-HCN1 might be transported retrogradely to other brain regions after infusion in the dorsal CA1 region, thus contributing alteration in behavioral outputs. We found, however, that there were no GFP expressions in other brain regions including the dorsal raphe containing serotonergic cell bodies and locus coeruleus containing noradrenergic cell bodies (data not shown), suggesting that anxiolytic- and antidepressant-like behaviors are due to knockdown of HCN1 channels in the dorsal hippocampal CA1 region. This is consistent with the reports that VSV-G pseudotyped lentivirus did not transport retrogradely in the brain (Louboutin, Reyes et al. 2007), suggesting local expression in the primary injection area.

Airan et al. reported that CA1 activity in the ventral hippocampus was increased in the animal model of depression, and then decreased by clinical antidepressant drugs (Airan, Meltzer et al. 2007). Furthermore, it has been reported that hippocampal theta oscillations spread along the septotemporal hippocampus, indicating propagation of neuronal activity (Lubenov and Siapas 2009). Thus, it might be possible to change CA1 activity in the ventral hippocampus after chronic knockdown of HCN1 channels in the dorsal hippocampus.

Recently, Chen et al. reported that ketamine, an NMDA receptor antagonist, inhibited HCN1 channels resulting in the reduction of total I_h conductance in cortical and

CA1 pyramidal neurons (Chen, Shu et al. 2009). A sub-anesthetic dose of ketamine produced early onset and long lasting therapeutic antidepressant effects in patients with treatment-resistant depression as well as in an animal model of depression (Berman, Cappiello et al. 2000; Li, Lee et al. 2010; Autry, Adachi et al. 2011). However, ketamine is also known as a psychotomimetic agent producing hallucination, delirium, and confusion (Webster and Walker 2006; Remerand, Couvret et al. 2007). In addition, chronic administration of clinical antidepressant drugs increased the risk of seizures in depressed patients (Peck, Stern et al. 1983; Alldredge 1999; Salzberg and Vajda 2001). In our VSD optical imaging and field potential recordings, we did not observe abnormal epileptic-like activity in the shRNA-HCN1-infected CA1 region. In conclusion, genetic silencing of HCN1 expression might provide a better alternative to existing pharmacological interventions for depression and anxiety.

GLOSSARY

Action potential (AP)

Cornu Ammonis 1 (CA1)

Cornu Ammonis 2 (CA2)

Cornu Ammonis 2 (CA3)

Cyclic adenosine monophosphate (cAMP)

Cyclic-nucleotide-binding domain (CNBD)

Central nervous system (CNS)

Dentate gyrus (DG)

Day post infusion (DPI)

Excitatory postsynaptic potential (EPSP)

Fiber volley (FV)

Forced swim test (FST)

Green fluorescence protein (GFP)

Hyperpolarization-activated, cyclic nucleotide–gated nonselective cation channels (HCN channels),

Hyperpolarization-activated cyclic nucleotide-gated current (I_h)

Membrane time constant (τ_m)

Open field test (OFT)

Postnatal 28/112 (P28/P112)

Paired pulse ratio (PPR)

RNA interference (RNAi)

Red fluorescence protein (RFP)

Resting membrane potential (RMP)

Stratum oriens (SO)

Stratum pyramidale (SP)

Stratum radiatum (SR)

Stratum lacunosum moleculare (SLM)

Short hairpin RNA (ShRNA)

Voltage sensitive dye (VSD)

References

Airan, R. D., L. A. Meltzer, et al. (2007). "High-speed imaging reveals neurophysiological links to behavior in an animal model of depression." Science **317**(5839): 819-823.

Alldredge, B. K. (1999). "Seizure risk associated with psychotropic drugs: clinical and pharmacokinetic considerations." Neurology **53**(5 Suppl 2): S68-75.

Amaral, D. G. and M. P. Witter (1989). "The three-dimensional organization of the hippocampal formation: a review of anatomical data." Neuroscience **31**(3): 571-591.

Autry, A. E., M. Adachi, et al. (2011). "NMDA receptor blockade at rest triggers rapid behavioural antidepressant responses." Nature.

Bai, F., X. Li, et al. (2001). "Intra- and interstrain differences in models of "behavioral despair"." Pharmacol Biochem Behav **70**(2-3): 187-192.

Ball, S. G., A. Kuhn, et al. (2005). "Selective serotonin reuptake inhibitor treatment for generalized anxiety disorder: a double-blind, prospective comparison between paroxetine and sertraline." J Clin Psychiatry **66**(1): 94-99.

Beaumont, V. and R. S. Zucker (2000). "Enhancement of synaptic transmission by cyclic AMP modulation of presynaptic Ih channels." Nat Neurosci **3**(2): 133-141.

Berman, R. M., A. Cappiello, et al. (2000). "Antidepressant effects of ketamine in depressed patients." Biol Psychiatry **47**(4): 351-354.

Borelli, K. G., M. J. Nobre, et al. (2004). "Effects of acute and chronic fluoxetine and diazepam on freezing behavior induced by electrical stimulation of dorsolateral and lateral columns of the periaqueductal gray matter." Pharmacol Biochem Behav **77**(3): 557-566.

Brager, D. H. and D. Johnston (2007). "Plasticity of intrinsic excitability during long-term depression is mediated through mGluR-dependent changes in I(h) in hippocampal CA1 pyramidal neurons." J Neurosci **27**(51): 13926-13937.

Brewster, A. L., Y. Chen, et al. (2007). "Quantitative analysis and subcellular distribution of mRNA and protein expression of the hyperpolarization-activated cyclic nucleotide-gated channels throughout development in rat hippocampus." Cereb Cortex **17**(3): 702-712.

Campbell, S. and G. Macqueen (2004). "The role of the hippocampus in the pathophysiology of major depression." J Psychiatry Neurosci **29**(6): 417-426.

Campbell, S., M. Marriott, et al. (2004). "Lower hippocampal volume in patients suffering from depression: a meta-analysis." Am J Psychiatry **161**(4): 598-607.

Chang, P. Y., P. E. Taylor, et al. (2007). "Voltage imaging reveals the CA1 region at the CA2 border as a focus for epileptiform discharges and long-term potentiation in hippocampal slices." J Neurophysiol **98**(3): 1309-1322.

Chen, C. A. and H. Okayama (1988). "Calcium phosphate-mediated gene transfer: a highly efficient transfection system for stably transforming cells with plasmid DNA." Biotechniques **6**(7): 632-638.

Chen, X., S. Shu, et al. (2009). "HCN1 channel subunits are a molecular substrate for hypnotic actions of ketamine." J Neurosci **29**(3): 600-609.
Colombo, M., T. Fernandez, et al. (1998). "Functional differentiation along the anterior-posterior axis of the hippocampus in monkeys." J Neurophysiol **80**(2): 1002-1005.
Cryan, J. F., A. Markou, et al. (2002). "Assessing antidepressant activity in rodents: recent developments and future needs." Trends Pharmacol Sci **23**(5): 238-245.
Degroot, A., S. Kashluba, et al. (2001). "Septal GABAergic and hippocampal cholinergic systems modulate anxiety in the plus-maze and shock-probe tests." Pharmacol Biochem Behav **69**(3-4): 391-399.
Degroot, A. and D. Treit (2002). "Dorsal and ventral hippocampal cholinergic systems modulate anxiety in the plus-maze and shock-probe tests." Brain Res **949**(1-2): 60-70.
Dembrow, N. C., R. A. Chitwood, et al. (2010). "Projection-specific neuromodulation of medial prefrontal cortex neurons." J Neurosci **30**(50): 16922-16937.
Dulawa, S. C., K. A. Holick, et al. (2004). "Effects of chronic fluoxetine in animal models of anxiety and depression." Neuropsychopharmacology **29**(7): 1321-1330.
Elbashir, S. M., J. Harborth, et al. (2001). "Duplexes of 21-nucleotide RNAs mediate RNA interference in cultured mammalian cells." Nature **411**(6836): 494-498.
Ennaceur, A., S. Michalikova, et al. (2010). "Distinguishing anxiolysis and hyperactivity in an open space behavioral test." Behav Brain Res **207**(1): 84-98.
File, S. E., L. E. Gonzalez, et al. (1998). "Endogenous acetylcholine in the dorsal hippocampus reduces anxiety through actions on nicotinic and muscarinic1 receptors." Behav Neurosci **112**(2): 352-359.
Frick, A. and D. Johnston (2005). "Plasticity of dendritic excitability." J Neurobiol **64**(1): 100-115.
Garza, J. C., M. Guo, et al. (2008). "Leptin increases adult hippocampal neurogenesis in vivo and in vitro." J Biol Chem **283**(26): 18238-18247.
Gould, N. F., M. K. Holmes, et al. (2007). "Performance on a virtual reality spatial memory navigation task in depressed patients." Am J Psychiatry **164**(3): 516-519.
Grishok, A., A. E. Pasquinelli, et al. (2001). "Genes and mechanisms related to RNA interference regulate expression of the small temporal RNAs that control C. elegans developmental timing." Cell **106**(1): 23-34.
Hu, H., K. Vervaeke, et al. (2002). "Two forms of electrical resonance at theta frequencies, generated by M-current, h-current and persistent Na+ current in rat hippocampal pyramidal cells." J Physiol **545**(Pt 3): 783-805.
Jacobi, F., H. U. Wittchen, et al. (2004). "Prevalence, co-morbidity and correlates of mental disorders in the general population: results from the German Health Interview and Examination Survey (GHS)." Psychol Med **34**(4): 597-611.
Kennedy, S. H., K. R. Evans, et al. (2001). "Changes in regional brain glucose metabolism measured with positron emission tomography after paroxetine treatment of major depression." Am J Psychiatry **158**(6): 899-905.

Lamers, F., P. van Oppen, et al. (2011). "Comorbidity patterns of anxiety and depressive disorders in a large cohort study: the Netherlands Study of Depression and Anxiety (NESDA)." J Clin Psychiatry **72**(3): 341-348.

Lewis, A. S., S. P. Vaidya, et al. (2011). "Deletion of the Hyperpolarization-Activated Cyclic Nucleotide-Gated Channel Auxiliary Subunit TRIP8b Impairs Hippocampal Ih Localization and Function and Promotes Antidepressant Behavior in Mice." J Neurosci **31**(20): 7424-7440.

Li, N., B. Lee, et al. (2010). "mTOR-dependent synapse formation underlies the rapid antidepressant effects of NMDA antagonists." Science **329**(5994): 959-964.

Liu, J., J. C. Garza, et al. (2010). "Acute administration of leptin produces anxiolytic-like effects: a comparison with fluoxetine." Psychopharmacology (Berl) **207**(4): 535-545.

Liu, Q., T. A. Rand, et al. (2003). "R2D2, a bridge between the initiation and effector steps of the Drosophila RNAi pathway." Science **301**(5641): 1921-1925.

Lorincz, A., T. Notomi, et al. (2002). "Polarized and compartment-dependent distribution of HCN1 in pyramidal cell dendrites." Nat Neurosci **5**(11): 1185-1193.

Louboutin, J. P., B. A. Reyes, et al. (2007). "Strategies for CNS-directed gene delivery: in vivo gene transfer to the brain using SV40-derived vectors." Gene Ther **14**(12): 939-949.

Lu, X. Y., C. S. Kim, et al. (2006). "Leptin: a potential novel antidepressant." Proc Natl Acad Sci U S A **103**(5): 1593-1598.

Lubenov, E. V. and A. G. Siapas (2009). "Hippocampal theta oscillations are travelling waves." Nature **459**(7246): 534-539.

Lucki, I. (1997). "The forced swimming test as a model for core and component behavioral effects of antidepressant drugs." Behav Pharmacol **8**(6-7): 523-532.

Ludwig, A., T. Budde, et al. (2003). "Absence epilepsy and sinus dysrhythmia in mice lacking the pacemaker channel HCN2." EMBO J **22**(2): 216-224.

Magee, J. C. (1998). "Dendritic hyperpolarization-activated currents modify the integrative properties of hippocampal CA1 pyramidal neurons." J Neurosci **18**(19): 7613-7624.

Magee, J. C. (1999). "Dendritic lh normalizes temporal summation in hippocampal CA1 neurons." Nat Neurosci **2**(6): 508-514.

Magee, J. C. (1999). "Dendritic voltage-gated ion channels. In: Dendrites." London: Oxford University Press p.139-155.

Mayberg, H. S. (1997). "Limbic-cortical dysregulation: a proposed model of depression." J Neuropsychiatry Clin Neurosci **9**(3): 471-481.

Mayberg, H. S. (2003). "Modulating dysfunctional limbic-cortical circuits in depression: towards development of brain-based algorithms for diagnosis and optimised treatment." Br Med Bull **65**: 193-207.

Mayberg, H. S., S. K. Brannan, et al. (2000). "Regional metabolic effects of fluoxetine in major depression: serial changes and relationship to clinical response." Biol Psychiatry **48**(8): 830-843.

Mayberg, H. S., A. M. Lozano, et al. (2005). "Deep brain stimulation for treatment-resistant depression." Neuron **45**(5): 651-660.

McCormick, D. A. and H. C. Pape (1990). "Properties of a hyperpolarization-activated cation current and its role in rhythmic oscillation in thalamic relay neurones." J Physiol **431**: 291-318.

McLaughlin, R. J., M. N. Hill, et al. (2007). "Local enhancement of cannabinoid CB1 receptor signalling in the dorsal hippocampus elicits an antidepressant-like effect." Behav Pharmacol **18**(5-6): 431-438.

Mineur, Y. S., C. Belzung, et al. (2006). "Effects of unpredictable chronic mild stress on anxiety and depression-like behavior in mice." Behav Brain Res **175**(1): 43-50.

Monteggia, L. M., A. J. Eisch, et al. (2000). "Cloning and localization of the hyperpolarization-activated cyclic nucleotide-gated channel family in rat brain." Brain Res Mol Brain Res **81**(1-2): 129-139.

Nadin, B. M. and P. J. Pfaffinger (2010). "Dipeptidyl peptidase-like protein 6 is required for normal electrophysiological properties of cerebellar granule cells." J Neurosci **30**(25): 8551-8565.

Narayanan, R. and D. Johnston (2007). "Long-term potentiation in rat hippocampal neurons is accompanied by spatially widespread changes in intrinsic oscillatory dynamics and excitability." Neuron **56**(6): 1061-1075.

Nolan, M. F., G. Malleret, et al. (2004). "A behavioral role for dendritic integration: HCN1 channels constrain spatial memory and plasticity at inputs to distal dendrites of CA1 pyramidal neurons." Cell **119**(5): 719-732.

Nolan, M. F., G. Malleret, et al. (2003). "The hyperpolarization-activated HCN1 channel is important for motor learning and neuronal integration by cerebellar Purkinje cells." Cell **115**(5): 551-564.

Notomi, T. and R. Shigemoto (2004). "Immunohistochemical localization of Ih channel subunits, HCN1-4, in the rat brain." J Comp Neurol **471**(3): 241-276.

Padovan, C. M. and F. S. Guimaraes (2004). "Antidepressant-like effects of NMDA-receptor antagonist injected into the dorsal hippocampus of rats." Pharmacol Biochem Behav **77**(1): 15-19.

Pape, H. C. (1996). "Queer current and pacemaker: the hyperpolarization-activated cation current in neurons." Annu Rev Physiol **58**: 299-327.

Peck, A. W., W. C. Stern, et al. (1983). "Incidence of seizures during treatment with tricyclic antidepressant drugs and bupropion." J Clin Psychiatry **44**(5 Pt 2): 197-201.

Piskorowski, R., B. Santoro, et al. (2011). "TRIP8b Splice Forms Act in Concert to Regulate the Localization and Expression of HCN1 Channels in CA1 Pyramidal Neurons." Neuron **70**(3): 495-509.

Poolos, N. P., M. Migliore, et al. (2002). "Pharmacological upregulation of h-channels reduces the excitability of pyramidal neuron dendrites." Nat Neurosci **5**(8): 767-774.

Porsolt, R. D., A. Bertin, et al. (1977). "Behavioral despair in mice: a primary screening test for antidepressants." Arch Int Pharmacodyn Ther **229**(2): 327-336.

Prut, L. and C. Belzung (2003). "The open field as a paradigm to measure the effects of drugs on anxiety-like behaviors: a review." Eur J Pharmacol **463**(1-3): 3-33.

Remerand, F., C. Couvret, et al. (2007). "[Prevention of psychedelic side effects associated with low dose continuous intravenous ketamine infusion]." Therapie **62**(6): 499-505.

Robinson, R. B. and S. A. Siegelbaum (2003). "Hyperpolarization-activated cation currents: from molecules to physiological function." Annu Rev Physiol **65**: 453-480.

Salzberg, M. R. and F. J. Vajda (2001). "Epilepsy, depression and antidepressant drugs." J Clin Neurosci **8**(3): 209-215.

Santoro, B., D. T. Liu, et al. (1998). "Identification of a gene encoding a hyperpolarization-activated pacemaker channel of brain." Cell **93**(5): 717-729.

Shah, M. M., A. E. Anderson, et al. (2004). "Seizure-induced plasticity of h channels in entorhinal cortical layer III pyramidal neurons." Neuron **44**(3): 495-508.

Sonawalla, S. B., A. Farabaugh, et al. (2002). "Fluoxetine treatment of depressed patients with comorbid anxiety disorders." J Psychopharmacol **16**(3): 215-219.

Stock, H. S., G. A. Hand, et al. (2001). "Changes in defensive behaviors following olfactory bulbectomy in male and female rats." Brain Res **903**(1-2): 242-246.

Stuart, G. J., H. U. Dodt, et al. (1993). "Patch-clamp recordings from the soma and dendrites of neurons in brain slices using infrared video microscopy." Pflugers Arch **423**(5-6): 511-518.

Thorne, R. G. and C. Nicholson (2006). "In vivo diffusion analysis with quantum dots and dextrans predicts the width of brain extracellular space." Proc Natl Acad Sci U S A **103**(14): 5567-5572.

Tominaga, T., Y. Tominaga, et al. (2000). "Quantification of optical signals with electrophysiological signals in neural activities of Di-4-ANEPPS stained rat hippocampal slices." J Neurosci Methods **102**(1): 11-23.

Vigna, E. and L. Naldini (2000). "Lentiviral vectors: excellent tools for experimental gene transfer and promising candidates for gene therapy." J Gene Med **2**(5): 308-316.

Wang, M., B. P. Ramos, et al. (2007). "Alpha2A-adrenoceptors strengthen working memory networks by inhibiting cAMP-HCN channel signaling in prefrontal cortex." Cell **129**(2): 397-410.

Webster, L. R. and M. J. Walker (2006). "Safety and efficacy of prolonged outpatient ketamine infusions for neuropathic pain." Am J Ther **13**(4): 300-305.

Zagotta, W. N. and S. A. Siegelbaum (1996). "Structure and function of cyclic nucleotide-gated channels." Annu Rev Neurosci **19**: 235-263.

Zhao, Y., K. Keating, et al. (2008). "Characterization of complete particles (VSV-G/SIN-GFP) and empty particles (VSV-G/EMPTY) in human immunodeficiency virus type 1-based lentiviral products for gene therapy: potential applications for improvement of product quality and safety." Hum Gene Ther **19**(5): 475-486.

Vita

Chung Sub Kim graduated with a B.A. in Microbiology from InJe University in 2001 and an M.S. in medical science from Yonsei University in 2003. He worked as a senior research assistant in pharmacology at University of Texas Health Science Center at San Antonio from 2003 to 2006. He joined the graduate program in Institute for Neuroscience at the University of Texas at Austin in August 2006.

E-mail address: ck4328@utexas.edu

This dissertation was typed by Chung Sub Kim